



HHS Public Access

Author manuscript

Immunity. Author manuscript; available in PMC 2024 December 26.

Published in final edited form as:

Immunity. 2023 October 10; 56(10): 2311–2324.e6. doi:10.1016/j.immuni.2023.08.001.

Mechanotransduction via Endothelial Adhesion Molecule CD31 Initiates Transmigration and Reveals a Role for Vascular Endothelial Growth Factor Receptor 2 in Diapedesis

Tao Fu^{*},
David P. Sullivan^{*},
Annette M. Gonzalez,
Maureen E. Haynes,
Prarthana J. Dalal,
Nakisha S. Rutledge,
Abigail L. Tierney,
Julia A. Yescas,
Evan W. Weber¹,
William A. Muller^{2,3}

Department of Pathology, Northwestern University Feinberg School of Medicine, Chicago, IL, USA

Summary

Engagement of platelet endothelial cell adhesion molecule 1 (PECAM, PECAM-1, CD31) on the leukocyte pseudopod with PECAM at the endothelial cell border initiates transendothelial migration (TEM, diapedesis). We show, using fluorescence lifetime imaging microscopy (FLIM), that physical traction on endothelial PECAM during TEM initiated the endothelial signaling pathway. In this role, endothelial PECAM acted as part of a mechanotransduction complex with VE-cadherin and vascular endothelial growth factor receptor 2 (VEGFR2); this predicted that VEGFR2 was required for efficient TEM. We show that TEM required both VEGFR2 and the ability of its Y1175 to be phosphorylated, but not VEGF or VEGFR2 endogenous kinase activity. Using inducible endothelial-specific VEGFR2-deficient mice, we show in three mouse models of inflammation that absence of endothelial VEGFR2 significantly (by 75%) reduced neutrophil extravasation by selectively blocking diapedesis. These findings provide a more complete understanding of the process of transmigration and identify several potential anti-inflammatory targets.

Graphical Abstract

²Corresponding Author.

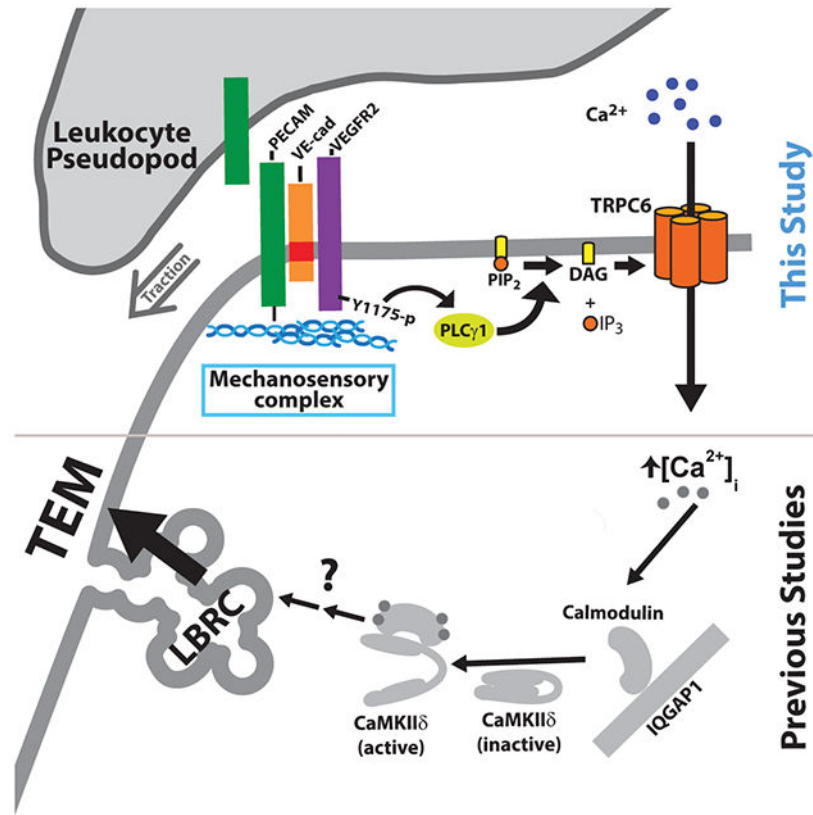
^{*}These authors contributed equally.

¹Present address: Department of Pediatrics, Perelman School of Medicine, University of Pennsylvania, Philadelphia, PA, USA

³Lead Contact

Declaration of Interests

The authors declare no competing interests.



Keywords

Mechanotransduction; VEGFR2; PECAM; Transmigration; Inflammatory Signaling

Introduction

We have known for three decades that an increase in endothelial cell free calcium ion concentration ($\uparrow[\text{Ca}^{2+}]_i$) is required for transendothelial migration (TEM) of leukocytes¹. Buffering intracellular calcium flux in endothelial cells leads to the inability of adherent neutrophils to transmigrate. At about the same time we have reported that interrupting homophilic interactions of leukocyte platelet endothelial cell adhesion molecule (PECAM) with endothelial cell PECAM leads to the same phenotype: neutrophils or monocytes tightly adherent to and apparently crawling along endothelial cell borders, but unable to transmigrate². These phenomena are directly connected. PECAM engagement on the endothelial cell activates the divalent cation channel transient receptor potential channel 6 (TRPC6), which is responsible for the increase in cytosolic free calcium ion ($\uparrow[\text{Ca}^{2+}]_i$) that is required for TEM³. siRNA silencing of TRPC6 or expression of dominant negative TRPC6 reduces TEM *in vitro*. Mice lacking TRPC6 in endothelial cells do not support efficient TEM, and the neutrophils are arrested on the apical surfaces of postcapillary venules *in vivo*³.

PECAM, TRPC6, and $\uparrow[\text{Ca}^{2+}]_i$ are co-localized spatially and temporally at the endothelial cell borders during TEM *in vivo* as well ^{3,4}. However, the mechanism by which PECAM activates TRPC6 has remained a mystery. Tzima *et al.* have described a mechanosensory complex in vascular endothelial cells consisting of PECAM, VE-cadherin, and vascular endothelial cell growth factor receptor 2 (VEGFR2) capable of responding to fluid shear over the cells and causing them to align in the direction of flow ⁵. We will refer to this as the PECAM mechanotransduction complex. The Martin Schwartz lab later has used PECAM molecules with embedded tension sensors ^{6,7} to demonstrate that PECAM has to be intact and able to sense tension in order for endothelial cells to respond to fluid flow ⁷. The tension sensor had been placed on the C-terminal side of the two ITIM domains required for PECAM signaling (containing Y663 and Y686). The negative control sensor had been missing the amino acids encoded by the final two exons of PECAM (exons 15 and 16), which are responsible for interaction with vimentin in the cytoskeleton and thus for generating tension across PECAM ⁷.

We hypothesized that the same complex is responsible for transducing tension on endothelial PECAM, thereby propagating the biochemical signal to initiate TEM. Here we report the discovery that PECAM on the leukocyte pseudopod, as it engages PECAM in the endothelial junction, activates the PECAM mechanotransduction complex, which converts this physical signal into a series of biochemical signals that enable TEM. Furthermore, our work demonstrates a previously undescribed role for VEGFR2 in transmigration *in vitro* and *in vivo*, which we show is ligand-independent *in vitro*.

Results

Cross-linking endothelial cell PECAM initiates calcium signaling for transmigration.

We have previously demonstrated that endothelial cell PECAM promotes TEM by activating the divalent cation channel TRPC6 to allow calcium influx for the $\uparrow[\text{Ca}^{2+}]_i$ required for TEM ³. PECAM and TRPC6 co-localize by immunofluorescence at the endothelial cell borders ³, which means that they may be within ~ 200 nm of each other. In order to better define their potential interactions, we performed a proximity ligation assay (PLA), which is theoretically capable of detecting proteins that are within ~ 40 nm of each other ⁸. Because there are no antibodies that recognize TRPC6 well in intact cells ³, human umbilical vein endothelial cells (HUVEC) expressing FLAG-tagged TRPC6 were incubated with anti-FLAG antibody, *anti*-PECAM antibody, or both, and the PLA signal was generated. Background in both of the single antibody controls was extremely low (Fig. 1 A, small panels), while a bright signal was seen along endothelial cell borders when both anti-PECAM and anti-FLAG were used, indicating that PECAM and TRPC6 were within 40 nm of each other interacting directly or as part of a larger protein complex (Fig. 1A).

Since activation of TRPC6 occurs downstream of endothelial cell PECAM engagement ³, we hypothesized that multivalent engagement of endothelial cell PECAM promoted by PECAM on the leukocyte pseudopod might initiate PECAM signaling in ECs. To mimic this, we tested whether cross-linking of endothelial cell PECAM would overcome the block to TEM imposed by anti-PECAM blocking antibodies, which prevent their ligation (schematic of expected effects shown in Fig. 1B). As shown in Fig. 1C and D for both PMN

and monocytes respectively, anti-PECAM blocked TEM across control (vehicle treated) endothelial monolayers to the same extent as buffering intracellular calcium with BAPTA, as demonstrated previously³. Cross-linking endothelial PECAM overcame the ongoing block and allowed essentially complete TEM within several minutes (Fig. 1). Endothelial cells pre-treated with BAPTA to buffer intracellular calcium prevented this effect, demonstrating that PECAM signaling requires $\uparrow[\text{Ca}^{2+}]_i$. These experiments show that antibody mediated cross-linking of endothelial PECAM activates the PECAM signaling pathway and leads to $\uparrow[\text{Ca}^{2+}]_i$, presumably via TRPC6. Combined with our previous data that directly activating TRPC6 via its specific activator Hyp9 will selectively overcome a block to endothelial PECAM in a similar manner to promote TEM³, this provides us with a way to synchronize PECAM signaling selectively on the endothelial cells to better dissect the pathway.

PECAM engagement activates Phospholipase C γ 1 through VEGFR2.

Diacylglycerol (DAG) is a natural activator of TRPC6 and treatment with a cell-permeable analogue of DAG, 1-Oleoyl-2-acetyl-*sn*-glycerol (OAG) can bypass the PECAM signaling step to initiate TEM³. Since DAG is produced by hydrolysis of phosphatidylinositol 4,5 biphosphate (PIP₂) into DAG plus inositol trisphosphate (IP₃) by the phospholipase C (PLC) family of enzymes, these observations suggest that PLC enzymes are critical regulators of TEM. To test this, we pre-treated endothelium with a broad-spectrum phospholipase C inhibitor U73122. This agent dose-dependently blocked neutrophil and monocyte TEM with 10 μM blocking as well as an optimal concentration of anti-PECAM mAb, with negligible effects on leukocyte adhesion (Fig. 1E-H). While there are always issues of specificity with pharmacologic blockade, eluate controls demonstrated there was apparently no significant carryover of the inhibitor that affected leukocytes (Fig. 1I).

These experiments showed that endothelial cell PLC was required for TEM. However, they did not demonstrate that PECAM engagement was required for its activation. Nor did it reveal which PLC isoform(s) were responsible for the production of DAG. The latter could be biologically important since the PLC β family is activated by G-protein coupled receptors, while the PLC γ family is activated by membrane tyrosine kinases. In order to identify the endothelial PLC isoform(s) responsible for mediating TEM, we cross-linked PECAM and performed Immuno blots on endothelial cell lysates probing for total and phosphorylated varieties of the most abundant endothelial cell PLC isoforms. PECAM cross-linking did not induce phosphorylation of PLC β 3 on serine 537 or serine 1105, its two sites of activation⁹ (Fig. 2A-D). However, we did observe phosphorylation of PLC γ 1 on tyrosine 783, the phosphotyrosine residue required for its lipase activity¹⁰, within 5 – 10 min. of cross-linking (Fig. 2E,F).

These data suggest that PIP₂ is hydrolyzed by PLC γ 1, but not PLC β 3, downstream of PECAM ligation. Since PLC γ 1 is known to be activated by receptor tyrosine kinases (RTK)¹¹, we hypothesized that the highly-expressed and junctional endothelial RTK, VEGFR2, may act downstream of PECAM to phosphorylate PLC γ 1. Indeed, PECAM cross-linking led to phosphorylation VEGFR2 on tyrosine 1175, the tyrosine responsible for activating PLC γ 1^{12,13}, already detectable at 3 min (not shown) and peaking by 5 min. (Fig.

2G,H). This time course is faster than phosphorylation of PLC γ 1, which is consistent with VEGFR2 being upstream of the phosphorylation of PLC γ 1.

The PECAM mechanotransduction complex on endothelium initiates TEM

Since cross-linking PECAM to mimic multivalent engagement by PECAM on the leukocyte pseudopod activated PLC γ 1 through VEGFR2, we wondered whether the PECAM mechanotransduction complex, located at the endothelial cell border⁵, might be involved. This complex is activated indirectly by Piezo-1 in response to fluid shear on the apical surface¹⁴. We hypothesized that for TEM, instead of being activated indirectly as in the case of fluid shear, the PECAM mechanotransduction complex might be activated directly by the physical traction of PECAM on the leukocyte, as it moves through the junction, with PECAM at the endothelial cell border. To test whether endothelial PECAM acts as part of a mechanosensing complex during TEM, we used PECAM molecules with embedded tension sensors developed by the Martin Schwartz lab^{6,7}. These constructs contain Venus and Teal Fluorescent Proteins connected by a flexible region such that when they are pulled apart, Forster Resonance Energy Transfer (FRET) was decreased and fluorescence lifetime was increased (see construct schematic and expected changes induced by tension in Fig. 3A. A negative control version was missing only the final 17 C-terminal amino acids encoded by exons 15 and 16 (15,16) so it did not anchor to vimentin in the endothelial cytoskeleton⁷ and hence could transmit tension across the PECAM molecule. Both versions were otherwise identical, and specifically both contained the critical ITIM motifs (surrounding Y663 and Y686) encoded by exons 13 and 14, respectively¹⁵.

In published studies, the human PECAM tension sensors have been expressed in bovine aortic endothelial cells or endothelial cell lines from PECAM-deficient mice⁷. To first validate their function in human endothelial cells, we silenced PECAM using shRNA in primary HUVEC and re-expressed PECAM with either the tension sensing version (TS) or the non-tension-sensing (15,16) version (Fig. 3B). These endothelial cells were then subjected to shear flow (11.5 dynes/cm²) on glass bottomed culture dishes for 48 hours as described¹⁶. As expected, control cells realigned in the direction of flow, whereas HUVEC in which PECAM was silenced did not (Fig. 3C,D). shRNA-silenced cells that were transfected to re-express TS PECAM aligned with flow, while those transfected to re-express 15,16 PECAM did not (Fig. 3C, D). In order to avoid any confounding effects of fluid shear on the PECAM/VE-cadherin/VEGFR2 mechanotransduction complex, our TEM experiments were carried out in the absence of flow under conditions that we have shown promote TEM of neutrophils and monocytes essentially as efficiently as under flow^{17,18}. We silenced PECAM in HUVEC grown on hydrated collagen gels and re-expressed the tension sensing or 15,16 PECAM in some monolayers. As expected, shRNA silencing of PECAM resulted in a large reduction of TEM. Re-expression of the tension-sensing PECAM construct restored TEM to baseline, while expression of the construct unable to sense tension had no effect (Fig. 3E).

The preceding experiments showed that a version of PECAM capable of transducing tension could promote TEM while a version of PECAM that could not transduce tension could not support TEM. Strictly speaking, however, that experiment did not demonstrate that

tension on PECAM occurred during TEM. To answer this question, we observed endothelial cells expressing those same constructs during neutrophil TEM using Fluorescence Lifetime Imaging Microscopy (FLIM). These experiments were carried out in the absence of fluid shear to eliminate that contribution to PECAM activation. Endothelial cells expressing the tension sensing version of PECAM showed a significant increase in the fluorescence lifetime of the TFP fluorophore during TEM (Fig. 3F,G), while those expressing the 15,16 version did not demonstrate a change in FLIM and did not support TEM (Fig 3E, F). These differences were significant and are in the range of changes in FRET⁷ and FLIM¹⁹ shown in previous publications for these molecules under tension.

Collectively, these experiments demonstrate that endothelial cell PECAM transduces force to mediate TEM. However, they do not show that PECAM is part of the PECAM mechanosensing complex. This complex requires all three components; elimination of any one of them renders the complex ineffective⁵. Therefore, we next tested the requirement for VE-cadherin in transducing mechanical force. Coon, et al. have shown that the mechanotransduction complex requires interaction of the VE-cadherin transmembrane domain with the transmembrane domain of VEGFR2 (or VEGFR3). A chimera of VE-cadherin containing the transmembrane domain of N-cadherin retained all the adhesive and barrier functions of VE-cadherin, but did not function in the tension sensing complex²⁰. We synthesized cDNAs to express the human versions of the corresponding VE-cadherin molecules (Fig. 4A). ShRNA silencing of VE-cadherin reduced TEM of monocytes (Fig. 4B) significantly. Re-expression of authentic (wild-type) VE-cadherin rescued TEM to baseline (Fig. 4B). However, re-expression of VE-cadherin containing the N-cadherin transmembrane domain was completely unable to restore TEM (Fig. 4B).

VEGFR2 is required for targeted recycling and TEM in a ligand-independent manner.

If the full mechanosensing apparatus is required for TEM, then functional VEGFR2 should be required as well. In fact, shRNA silencing of VEGFR2 significantly blocked TEM and re-expression of wild-type VEGFR2 completely restored TEM, ruling out off-target effects (Fig. 5A,B). However, attempts to rescue TEM using a VEGFR2 construct in which tyrosine 1175, the tyrosine required for activating PLC γ 1, was mutated to a phenylalanine (Y1175F) had no effect, showing that phospho-Y1175 was required for the role of VEGFR2 in transmigration (Fig. 5A,B).

We perform our TEM assays in the absence of serum, and our endothelial cells were cultured in adult human serum, which has low concentrations of VEGF. Nevertheless, it was possible that trace amounts of VEGF remained in the collagen gels on which the endothelial cells were plated. To determine whether the role of VEGFR2 was dependent on binding VEGF, we ran the experiment under our standard conditions with or without 10 μ g/ml of the VEGF neutralizing antibody bevacizumab (Avastin). There was no difference in neutrophil transmigration, indicating that the role of VEGFR2 in TEM was ligand-independent (Fig. 5C). Control experiments demonstrated that bevacizumab at that concentration blocked activation of VEGFR2 by VEGF (Fig. 5D).

To determine whether endogenous kinase activity was required for phosphorylation of VEGFR2, we studied the effect of the VEGFR2 kinase inhibitor SU1498 on TEM. Doses

of 1 μ M and 10 μ M, which clearly blocked phosphorylation of VEGFR2 tyrosine 1175 by VEGF (Fig. 5D), had no effect on TEM (Fig. 5E). In addition, we replaced WT VEGFR2 with a kinase-dead (K-D) version²¹. Endothelial cells expressing the K-D VEGFR2 still phosphorylated VEGFR2 on Y1175 when PECAM was crosslinked (Fig. 5F) and still promoted TEM (Fig. G). Control experiments showed that K-D VEGFR2 did not phosphorylate Y1175 when exposed to VEGF (Fig. 5H). Therefore, endogenous VEGFR2 kinase activity was not required for phosphorylating Y1175, consistent with a ligand-independent role for VEGFR2 in TEM. Identification of the kinase responsible for activation of VEGFR2 under these conditions is beyond the scope of this study. However, we have previously shown that src family kinase activity is required for TEM in our system²² and src kinases have been implicated in PECAM mechanotransduction activity under fluid shear sensing conditions^{5,14}. Consistent with this, preincubation of EC monolayers with the src kinase family inhibitor PP2, but not its inactive analogue PP3, significantly inhibited TEM (Fig. 5I).

In the response to fluid shear stress, Piezo 1, a mechanosensing channel, is involved in activating the PECAM mechanotransduction complex¹⁴. To determine whether Piezo 1 could also be responsible for the $\uparrow[\text{Ca}^{2+}]_i$ downstream of PECAM signaling for TEM, we repeated an experiment we had performed with TRPC6³. When endothelial PECAM signaling is interrupted by anti-PECAM mAb to prevent leukocyte PECAM engagement, TEM can be restored by cross-linking the antibody (Fig. 1) or directly activating TRPC6³. We repeated the latter experiment with direct activators of TRPC6 and Piezo 1 (Fig. 5E). Anti-PECAM mAb hec7 blocked TEM as expected, and this block could be overcome by providing the specific TRPC6 activator Hyp9 during the final 5 minutes of the TEM assay (Fig. 5E). However, in the same experiment, adding the Piezo 1 activator YODA1 had no effect on TEM at concentrations used in the literature (Fig. 5E). To show that YODA1 was indeed active at that concentration, we tested its ability to promote $\uparrow[\text{Ca}^{2+}]_i$ in endothelial cells loaded with the calcium-sensing fluorescent dye Fluo4. Addition of 5 – 10 μ M YODA1 to endothelial cells led to a rapid increase in intracellular calcium ion, as reported by the increased fluorescence in the Fluo4-loaded cells (Fig. 5J and Supplemental Videos 1-3).

Finally, if VEGFR2 were critically involved in the canonical signaling pathway for PECAM in TEM, shRNA silencing of VEGFR2 should interrupt targeted recycling of the lateral border recycling compartment (LBRC) to the site of transmigration. The LBRC is a reticulum of interconnected tubulo-vesicular membrane present along the endothelial cell border immediately below the junctional membrane²³. When a leukocyte transmigrates, membrane from the compartment is delivered in a bolus along microtubules in a kinesin-dependent manner, providing additional membrane surface area and unligated adhesion and signaling molecules to the leukocyte for efficient TEM²⁴. Anything that blocks this “targeted recycling” blocks TEM, including genetic deletion or interference with PECAM or any molecule in its signaling pathway^{3,4,23,25-27}. Since PECAM activation of TRPC6 was demonstrated to be necessary for targeted recycling and TEM³, shRNA silencing of VEGFR2 should interfere with targeted recycling as well. We measured targeted recycling with an assay that arrests leukocyte TEM shortly after it is initiated and labels membrane from the LBRC that is brought to the site of TEM²³. Recycled LBRC membrane is enriched around the leukocytes that have initiated TEM within that short time²³. ShRNA silencing

of VEGFR2 blocked targeted recycling of the LBRC, consistent with its block of neutrophil TEM (Fig. 5K,L). Targeted recycling and TEM were rescued when WT VEGFR2 was re-expressed in these endothelial cells, but not when the Y1175F mutant of VEGFR2 was re-expressed (Fig. 5K,L).

VEGFR2 is Required for Transendothelial Migration of Neutrophils *in vivo*.

Our findings *in vitro* demonstrated a ligand-independent role for VEGFR2 in TEM as part of the PECAM mechanotransduction complex. To our knowledge, a direct role for VEGFR2 in transendothelial migration of leukocytes has never been identified. To directly test whether VEGFR2 is a critical regulator of TEM *in vivo*, we bred conditional VEGFR2-deficient mice by mating endothelial cell specific inducible Cre mice (*Cdh5*(PAC)-CreERT2²⁸) with *Flk-1*^{fl/fl} mice²⁹. The offspring were bred to homozygosity for the *Flk-1*^{fl/fl} alleles and were healthy and normal when unstressed. Daily treatment with tamoxifen (2 mg in corn oil) intraperitoneally (i.p.) for 5 days, led to elimination of detectable VEGFR2 on isolated lung endothelial cells one week later. Littermates treated with vehicle (corn oil) only, expressed normal amounts of VEGFR2 (Fig. 6A).

Inducible endothelial-specific VEGFR2 deficient mice were treated with tamoxifen in corn oil or corn oil alone as described above and then rested for two weeks. They were then subjected to croton oil dermatitis (See Methods). Briefly, one ear of each mouse was painted with 20 μ l of 1% croton oil, an irritant, in a 4:1 mixture of acetone:olive oil and the contralateral ear was painted with the carrier alone, serving as a negative control for each mouse. Five to six hours later, the mice were sacrificed, ears harvested, fixed, and split into halves for immunofluorescence staining. Whole mounts were examined by confocal microscopy. The ears of mice that received croton oil became red and swollen shortly after the application, whereas the contralateral ears remained unchanged. The same total number of neutrophils were recruited to the ears of the mice independent of VEGFR2 expression (Fig. 6B,C). However, mice lacking VEGFR2 exhibited a profound defect in neutrophil extravasation wherein 80% of imaged neutrophils were apparently adherent to the luminal endothelial surface but were unable to cross, in contrast to 80% neutrophil extravasation in control mice.

To determine whether the effect of VEGFR2 deficiency on PMN transmigration lasted longer than six hours, we turned to a mouse model of aspiration pneumonia in which PMN predominate for the first 24 hours. Dilute hydrochloric acid was instilled into the trachea of anesthetized tamoxifen inducible VEGFR2 deficient mice that had been fed tamoxifen chow or control chow for 3 weeks. Twenty four hours later, mice were euthanized and bronchoalveolar lavage fluid was collected. Leukocyte numbers and subtypes were determined as described in Methods. The VEGFR2-deficient mice had a clear defect in neutrophil (Fig. 6E) and monocyte (Fig. 6F) migration into the injured lungs.

The dermatitis model offers a high-resolution evaluation of the position of neutrophils in relation to vasculature, but it is a snapshot in time. To visualize the interactions of neutrophils with the vasculature during the inflammatory response in living mice, we subjected the mice to intravital microscopy. We visualized the response to IL-1 β in the cremaster muscle bed as we have described previously^{4,27,30}. In the littermates receiving

corn oil only, there was robust PMN rolling, adhesion, and transendothelial migration out of the postcapillary venules into the interstitial tissue (Fig. 7 and Supplemental Video 4). In contrast, while rolling flux and leukocyte adhesion were not significantly affected in mice lacking VEGFR2 in their endothelium, transendothelial migration was decreased about 7-fold (Fig. 7 and Supplemental Video 5). Thus, VEGFR2 is required specifically for transmigration, but not earlier steps in extravasation *in vivo*. This is similar to the role of PECAM, and is consistent with VEGFR2 functioning in the mechanotransduction complex along with PECAM.

Discussion

Our data has shown that PECAM functions directly as part of a mechanotransduction complex to initiate transendothelial migration. Homophilic interactions of PECAM on the leukocyte pseudopod with PECAM concentrated at the endothelial cell border has long been known to be critical for TEM^{2,23,31,32}. Here, we demonstrated that engagement of leukocyte PECAM with endothelial cell PECAM produced tensile force, which in turn stimulated the signals on the endothelial cell that lead to TEM. We hypothesize that this occurs through traction on endothelial PECAM as the pseudopod attempts to advance into the junction. This is true for both neutrophils and monocytes, which seem to rely to the same extent on this signaling function, although PMN transmigrate more rapidly under our *in vitro* conditions.

PECAM has previously been demonstrated to be a mechanosensitive molecule in response to fluid shear. Fujiwara's group has shown that direct mechanical stimulation of PECAM using fluid shear³³ or magnetic beads coated with anti-PECAM antibody³⁴ result in phosphorylation of PECAM on the cytoplasmic tail and PECAM-dependent phosphorylation of extracellular signal-regulated kinase (ERK). Tzima, *et al.* have further defined PECAM signaling in response to fluid shear, identifying a "mechanosensory complex" consisting of PECAM, VE-cadherin, and VEGFR2; all three of which are required for cells to align in response to fluid shear via a mechanism involving activation of PI₃K and activation of integrins⁵. The Martin Schwartz group has produced PECAM and VE-cadherin tension sensor constructs and have demonstrated that response to fluid shear involves a decrease in tension on VE-cadherin, an increase in tension on PECAM⁷, and the binding of transmembrane domain of VE-cadherin to VEGFR2²⁰. The sensing of tension by these constructs relies on binding of the cytoplasmic tail of PECAM to vimentin⁷. Whether vimentin plays the same role in maintaining tension across PECAM during TEM is not known, but is the subject of ongoing research in our lab. Otte, *et al.*, has presented evidence that PECAM forms a complex with G $\alpha_{q/11}$ that dissociates upon rapid changes in shear stress³⁵. Offermanns' group further has refined this showing that the PECAM mechanotransduction complex, the G $\alpha_{q/11}$ -containing purinergic receptor P2Y₂, and the mechanosensor Piezo 1 are all involved in sensing both laminar and disturbed flow¹⁴. The end result of the mechanotransduction pathway in response to flow is to activate integrins on the basal surface of the endothelial cell to realign the cells along the vector of fluid shear.

Despite prior work demonstrating PECAM to be involved in mechanotransduction of fluid shear, the PECAM-containing mechanosensory complex had not been thought to be involved in regulating TEM. By performing critical experiments in the absence of fluid shear, we

avoided the confounding effects of the response of the same complex to Piezo 1 and fluid shear. We show that rather than indirectly sensing fluid shear via Piezo 1, direct physical tension on endothelial cell PECAM during TEM engaged the PECAM mechanotransduction complex. This activated a different pathway—one that led to $\uparrow[\text{Ca}^{2+}]_i$ through the TRPC6 cation channel and targeted recycling of the LBRC to promote TEM.

Recent work demonstrates that Piezo1 is required for leukocyte transmigration *in vitro* and *in vivo*³⁶. Even more recently, a fraction of Piezo 1 has been shown to interact with PECAM at cell borders, although the interaction with PECAM decreases Piezo 1 channel activity³⁷. Since Piezo1 has also been implicated in initiating response to fluid shear via the PECAM mechanotransduction complex¹⁴, we went back and examined whether Piezo1 served as a mechanosensor to allow $\uparrow[\text{Ca}^{2+}]_i$ downstream of PECAM ligation. As we had shown previously³, blockade of TEM by anti-PECAM mAb could be overcome by direct activation of TRPC6 by the selective activator Hyp9, which restored the missing signal. However, the same dose of the Piezo1-specific activator Yoda1 used in the cited study (Ref. 36), did not overcome the anti-PECAM block. Control experiments showed that Yoda1 at this concentration was perfectly capable of activating $\uparrow[\text{Ca}^{2+}]_i$ in these endothelial cells. Just as increasing intracellular calcium ion by histamine did not overcome an anti-PECAM block, nor did activation of TRPC6 prior to engagement of PECAM³, these experiments show that TEM is not regulated by general increases in endothelial $[\text{Ca}^{2+}]$. Rather, the physiologic response to increases in calcium in TEM is dependent on the endothelial cell molecules controlling TEM at that point in time and space⁴.

The effect of Piezo1 on TEM requires fluid shear and traction on ICAM-1³⁶. ICAM-1 is involved in the locomotion step of extravasation³⁸ and concentrates under the leukocyte prior to diapedesis³⁹. The role of PECAM in the initiation of diapedesis, a slightly later stage in the process, does not require fluid shear, nor does the role of TRPC6 in mediating $\uparrow[\text{Ca}^{2+}]_i$, since both work efficiently in TEM under static conditions *in vitro*^{2,3,24} (and this paper) as well as under conditions of flow *in vivo*^{2,3,24}. Mice with endothelial cells selectively deficient in TRPC6 have a defective inflammatory response, with neutrophils arrested over endothelial borders, similar to mice in which PECAM is blocked with antibody³⁰ or whose endothelial cells are selectively defective in PECAM⁴⁰ or any of the molecules proximal to or distal to (refs^{4,27}) TRPC6 in the PECAM signaling pathway for TEM. What is most likely is that Piezo1 and TRPC6 operate in series, each supplying the calcium flux for sequential steps in the extravasation cascade. Both are necessary; yet neither is sufficient.

As part of this process, we showed a positive role for VE-cadherin in promoting TEM, whereas studies to date show that VE-cadherin plays a “negative” role in transmigration. Lusinskas and colleagues have shown that VE-cadherin leaves the site of diapedesis during TEM⁴¹. Vestweber’s group has shown that mutating VE-cadherin so that it could not leave the junction blocks TEM⁴². Therefore, it might not be expected that depletion of VE-cadherin would decrease TEM. We previously have demonstrated that PECAM-dependent targeted recycling of the LBRC precedes the loss of VE-cadherin from the cell border¹⁸. An explanation that fits all the data is that VE-cadherin first acts along with PECAM in the mechanosensory complex to promote activation of TRPC6, then leaves the site of TEM when the LBRC arrives. This explanation could also reconcile the decrease in tension across

VE-cadherin during response to fluid shear reported by the Schwartz group^{7,43} with the increase in tension across VE-cadherin during TEM reported by the Vestweber group¹⁹.

Of note, VE-cadherin is excluded from the LBRC^{44,45}. The PECAM mechanotransduction complex at the junction surface interacts with PECAM on the leukocyte to signal targeted recycling from within the cell. Our data show that the membrane compartments mix and yet VE-cadherin is actively excluded from the LBRC by trans-homophilic interactions⁴⁵. Whether there is a stable pool of tension signaling complex at the surface is not known.

Of major interest, we show a ligand-independent function for VEGFR2 in promoting TEM. VEGFR2 has not been implicated in TEM previously. Coon et al. has shown that as part of the response to fluid shear, VEGFR2 is phosphorylated on Y1175²⁰. We showed that in response to traction on endothelial PECAM, VEGFR2 was phosphorylated on Y1175, the phosphotyrosine required for activation of PLC γ 1^{12,13}, which in turn is required for the liberation of DAG to activate calcium flux through TRPC6 for TEM^{3,4}. Phosphorylation of Y1175 did not require endogenous VEGFR2 kinase activity, since TEM was not blocked by concentrations of the selective VEGFR2 kinase inactivator SU1498 at concentrations that clearly blocked activation of VEGFR2 by VEGF and a kinase-dead form of VEGFR2 was perfectly capable of supporting TEM. The activation of the PECAM mechanotransduction complex has been reported to require Src-family kinase activity⁵. We have previously shown phosphorylation of PECAM by Src-family kinase is required for TEM^{22,46}. However, the precise Src family kinase(s) implicated in the PECAM mechanotransduction complex is currently unknown and is the subject of future investigation.

It is tempting to speculate that during the evolution of the inflammatory response nature took advantage of the fluid shear sensing pathway that probably already existed in endothelial cells. Leukocytes that bear PECAM on their surface and had migrated to an endothelial cell border could engage endothelial cell PECAM in a multivalent manner and induce traction upon it, thus stimulating the mechanotransduction complex. Among the signaling pathways activated by VEGFR2, phosphorylation of PLC γ 1 would have led to elevated local concentrations of DAG that promote $\uparrow[\text{Ca}^{2+}]_i$ through TRPC6 and the calcium-dependent signaling pathways shown to be responsible for TEM downstream of PECAM^{4,27}.

A ligand-independent role for VEGFR2 in the PECAM signaling pathway is not incompatible with the VEGF dependent role for VEGFR2 in inflammatory angiogenesis, as these processes are taking place in different EC at anatomically distinct places in the vasculature. In some sense, the role of VEGFR2 in TEM may be thought to be the primary role of VEGFR2 in inflammation, since inflammatory angiogenesis does not take place until after leukocytes have crossed blood vessels. Our identification of a ligand-independent role for VEGFR2 in TEM suggests this may be an unexpected target for anti-inflammatory therapy that would not interfere with the angiogenic functions of VEGFR2.

Limitations of Study

We have not identified the specific kinase(s) responsible for activating VEGFR2 in this mechanotransduction system beyond the fact that it appears to be a *src* family kinase. Since PECAM-PECAM interactions initiate TEM, our experiments do not define whether the

PECAM mechanotransduction complex is required for the entire transmigration process or just for initiating it. Tension across PECAM is mediated by adhesion to vimentin when the PECAM mechanotransduction complex reacts to fluid shear. We do not know whether anchoring to vimentin plays the same role when the complex is involved in TEM. Finally, although we show a ligand-independent role in transmigration for VEGFR2 *in vivo* that is predicted from our *in vitro* experiments, we cannot carry out live animal experiments in the absence of VEGF, and our actual tension sensing measurements could only be conducted *in vitro*.

STAR Methods

RESOURCE AVAILABILITY

Lead Contact—Further information and requests for resources and reagents should be directed to and will be fulfilled by the lead contact, William Muller (wamuller@northwestern.edu).

Materials availability—Requests for plasmids generated and mouse lines generated in this study will be fulfilled by the lead contact, William Muller (wamuller@northwestern.edu).

Data and code availability—All data reported in this paper will be shared by the lead contact upon request. This paper does not report original code. Any additional information required to reanalyze the data reported in this paper is available from the lead contact upon request.

EXPERIMENTAL MODEL AND SUBJECT DETAILS

Mice—All experiments with animals were performed using protocols approved by Northwestern University's Institutional Animal Care and Use Committee (PHS assurance number A328301). Mice were housed in the institute's animal facility managed by the Center for Comparative Medicine and were maintained according to standard AAALAC methods. All experiments used adult mice 8-12 weeks old, which were age and sex-matched for each experiment. The *LysM-GFP VEGFR2^{flox/flox} Cad5-CreERT2* mouse line was generated by crossing FVB *LysM-eGFP* mouse strain (described in ³⁰) with the *VEGFR2^{flox/flox}* (obtained from Susan Quaggin, Northwestern) and C57Bl/6 *Cdh5-CreERT2* obtained from Dr. Ralf Adams at the Max Planck Institute and has been described previously ²⁸.

Cell lines—All procedures involving human subjects and human materials were approved by the Institutional Review Board of Northwestern University Feinberg School of Medicine. Human Umbilical Vein Endothelial Cells (HUVEC) were isolated from human umbilical cords as previously described ^{47,52}. At their second passage, isolated HUVEC were either cultured on three-dimensional type I collagen matrices (PureCol, Inamed Biomaterials, Fremont, CA) (described in ⁵²) and allowed to reach confluence before use (typically 2-3 days after seeding) to ensure the formation of high quality basement membranes. PBMCs and PMNs were harvested as described previously ^{52,53}.

METHOD DETAILS

Antibodies and reagents—The non-function blocking mouse anti-human PECAM antibody (clone P1.1³²) was purified from ascites generously gifted by Peter Newman (Blood Center of Wisconsin). This was then digested to F(ab) fragments using standard protocols. Rat anti-mouse PECAM (clone 390) and goat anti-Armenian hamster IgG were directly conjugated with Dylight 550 (Thermo Fisher Scientific) according to the manufacturer's protocols.

Cloning and Adenoviral preparation—We used the full-length VEGFR2 mCherry construct obtained from Addgene (plasmid#108854) as a template for cloning VEGFR2 into the pENTR4 GFP vector using the following primers: VEGFR2 Forward 5' – GCAAGAGCTCACCATGCAGAGCAAGGTGCTGCTG-3; VEGFR2 Reverse Primer: 5' – GTCCGAATTTCGAACAGGAGGAGAGCTCAGTGTG-3'. We mutated tyrosine residue position 1175 to phenylalanine using PCR site-directed mutagenesis using VEGFR2 pENTR4 GFP construct as a template with the following primers: VEGFR2 (Y1175F) Forward : phosphorylated 5' – TCATTGTTCTTCCGATATCAGAGACTTTGAGCATGG-3'; VEGFR2 (1175F) Reverse: phosphorylated 5' – AGTCTTTGCCATCTGCTGAGCATTAGCTTGCAAGAG-3'; The VEGFR2 Kinase Dead construct (VEGFR2 K-D) was generated using PCR site-directed mutagenesis and the VEGFR2 pENTR4 GFP construct as a template with the following primers: VEGFR2 (Y1054F,Y1059F) Forward: 5' - phosphorylated TTAAAGATCCAGATTTTGTGAGAAAAGGAGATGCTCGC-3'; VEGFR2 (Y1054F, Y1059F) Reverse: 5' - phosphorylated AAATATCCCGGGCCAAGCCAAAGTCACAGATTTTAAC-3'. The VE-cadherin chimera containing the N-cadherin transmembrane domain (VECadTMD) was generated by using the VE-cadherin(WT) GFP pENTR4 construct as a template which was previously described in¹⁸. The following primers were used to replace the transmembrane domain of VE-cadherin (amino acids: 717-747) with the transmembrane domain of N-cadherin: VECadherinTMD Forward: phosphorylated 5' – CTCTGCATCATCATCTGCTTATCCTTGTGCTGATGTTTGTGGTATGGATGAAACGG CGGCGGCTCCGGAAGCAGGCC-3'; VECadherinTMD Reverse: phosphorylated 5' – CAGGATGGCAATGATGGCACCGGTGCCAAGCCCCGCCACCTGGGCGGCCATATCC TC-3'; The PECAM tension sensors were a kind gift from Martin Schwartz and are described in⁷. We used these constructs as templates and cloned them into the pENTR4 entry vector by PCR using the following primers: PECAM Forward: 5' – ACGCAAAAGCTTACCATGCAGCCGAGGTGGGCC-3'; Reverse: 5' – GTCCGACCCGGGAAGTCCATCAAGGGAGCC -3'

We used the BlockiT pENTR/U6 entry vector and pAd/Destination Vector Gateway system (Invitrogen Corp., Carlsbad, CA) to generate shRNA adenovirus to target the 3-UTR region of VEGFR2 and PECAM. The $\alpha 6$ integrin shRNA BlockiT pENTR/U6 entry vector described in⁵⁴ was used as a template. Using PCR site-directed mutagenesis, we designed primers to replace the region corresponding to $\alpha 6$ integrin shRNA with VEGFR2 shRNA using the following primers: VEGFR2 Forward sh1: 5'-phosphorylated- AATCAAATGCGGCTACTTCCTGCTTTTTTCTAGACCCAGCTTTCTGTACAAAGTT

G-3; VEGFR2 Reverse sh1: 5' phosphorylated-CGTCAAATGCGGCTACTTCTGCGGTGTTTCGTCCTTTCCACAAGATATAT-3'. We used a similar approach to generate PECAM shRNA. We replaced a6 integrin shRNA with the following primers: PECAM shRNA Forward: 5' - phosphorylated AACTATTGAGAGACTGTCCTTGTCTTTTCTAGACCCAGCTTCTTGTACAAAGTTG-3'; PECAM shRNA Reverse: 5' -phosphorylated -CGCTATTGAGAGACTGTCCTTGTGCGGTGTTTCGTCCTTTCCACAAGATATAT-3' The VE-cadherin shRNA lentivirus construct was a kind gift from Dr. Alejandro Adam (Albany Medical College, Albany, NY). It has a targeted sequence directed against the 3'UTR 4024 AGTAATTGCTCTACAGATA (based on the first nucleotide of refseq NM_001795.3). Lentivirus was generated by standard procedures. The full-length, N-terminally FLAG-tagged wild-type TRPC6 (WT-T6) and dominant-negative TRPC6 (DN-T6) constructs were generously provided by Johannes Schlondorff (Beth Israel Deaconess Medical Center, Boston, MA)⁵¹.

These vectors were recombined with the adenoviral vector pAd/PL-DEST or pAd/CMV-V5 for the shRNA and reexpression constructs (respectively, both from Life Technologies) using LR clonase (Life Technologies) according to the manufacturer's guidelines and used to produce adenovirus for transduction according to standard methods⁵⁵.

shRNA depletion and transduction—For HUVEC protein depletion and viral transduction, all samples were prepared similarly. Briefly, adenovirus containing shRNA constructs were added one day after seeding in M199 with 2% FBS. The next day, the cells were washed and incubated with adenovirus containing reexpression constructs in M199 with 2% FBS. The following day, cells were washed and incubated with complete media for two days before being used. The amount of virus needed to achieve protein expression for each construct that was comparable to its endogenous protein expression was determined empirically for each construct. For all TEM experiments, HUVEC were activated with 20 ng/ml recombinant TNF α in conditioned media for at least 4 h before the start of the assay.

Proximity Ligation Assay (PLA)—PLA was conducted per manufacturer's instructions. Briefly, HUVEC monolayers plated on coverslip dishes (Mattek, Ashland, MA) were transduced with FLAG-TRPC6 for 72 h. Monolayers were fixed in 4% PFA for 10 min and permeabilized with 0.1% triton-X for 10 min. After extensively washing the monolayers, blocking buffer (5% BSA, 5% FBS, 5% NGS) was added for 30 min at room temperature. Next, primary antibody suspended in blocking buffer was added to monolayers overnight at 4°C. Species-specific IgG were used as negative controls. The next day, monolayers were washed and incubated with PLA secondary probes at 37°C for 1 hour. Ligation and amplification steps were subsequently completed at 37°C for 30 minutes and 100 min, respectively. After extensive washing, confocal images were visualized using an Ultraview Vox imaging system (Waltham, MA) equipped with a Yokogawa CSU-1 spinning disk. Images were acquired with a 40x oil immersion objective using Volocity software (Perkin Elmer, Waltham, MA). All images were processed and analyzed with ImageJ software (version 1.53q, NIH, Bethesda, MD).

PECAM Cross-Linking Experiments in the absence of leukocytes.—To mimic the multivalent engagement of leukocyte PECAM with endothelial PECAM, we first added anti-PECAM mAb hec7 or non-blocking anti-VE-cadherin mAb isotype control (hec1), both at 20 µg/ml to HUVEC monolayers, which were subsequently washed free of unbound antibody. Since most commercially available secondary antibodies recognize the constant region of the target heavy chain, intact mAb had to be used to obtain good cross-linking. F(ab')₂ fragments of Goat anti-mouse IgG antibody were added for the indicated times before washing and preparing for Western Blot.

Western Blotting—HUVEC or iHUVEC were grown on collagen gels and transduced as indicated and described above. After washing with PBS, the cells were lysed in 50 µl PBS containing 1% NP-40, 1x protease inhibitor cocktail (Sigma-Aldrich, P8340), and 1 mM PMSF (Sigma-Aldrich) for 5 min at RT. The lysates were collected and pooled from 2 wells, mixed with 6x Laemmli loading buffer with β-mercaptoethanol, and heated at 60°C for 30 min. Equivalent amounts were loaded onto a 8% polyacrylamide gel and resolved using SDS-PAGE. Proteins were transferred to PVDF and detected using standard western blotting techniques.

Immunofluorescence Microscopy—Confluent HUVEC or iHUVEC were fixed in 2% paraformaldehyde for 20 min, washed three times with PBS and blocked with blocking buffer (PBS with 5% BSA (Fraction V, Thermo Fisher Scientific) and 1% goat serum) for 30 min at room temperature (RT). Cells were then incubated with primary antibody at 10 µg/mL in blocking buffer for 45 min at RT, washed extensively with PBS, and then incubated with secondary antibody at 4 µg/mL in blocking buffer for 45 min at RT protected from light. For the visualization of protein localization, cells were permeabilized before blocking for 4 min with 0.1% Triton X-100 (Millipore Sigma). Confocal images (all figures unless otherwise noted) were collected using an Ultraview VoX imaging system (Waltham, MA) equipped with a Yokogawa CSU-1 spinning disk. Images were acquired with a 40× oil objective (NA 1.0) using Volocity software.

Fluorescence Lifetime Imaging Microscopy—HUVEC were grown on 35 mm plastic tissue culture dishes and transduced with the indicated adenovirus to express the PECAM tension sensor (PECAM TS) or the PECAM tailless control (PECAM 15, 16) for three days. PMNs were harvested as described above, labeled for 5 min with CellTracker Deep Red Dye, washed, and resuspended in M199 with 0.2% HSA to 4 x 10⁶ cells/ml. Monolayers were stimulated with 20 ng/ml recombinant TNFα overnight before being incubated with 2 x 10⁶ PMNs. After 10 min to allow for TEM to proceed partially, monolayers were rapidly washed and fixed with 4% PFA for 10 min and stored in PBS. Fluorescence Lifetime Imaging Microscopy (FLIM) images of endothelial cells with PMNs in TEM were captured on a Leica DiveB Sp8, an upright multiphoton microscope equipped with a Leica HC IRAPO L 25x motCORR water immersion lens (NA=1.00). PMNs and PECAM constructs were visualized using a Spectra Physics Mai Tai laser tuned to 840 nm and a Leica 4Tune detector using cutoffs of 460-500 nm (to detect PECAM construct TFP for FLIM) and 645-750 nm (to detect PMNs). The microscope was driven by Leica Application Suite X software version 3.5.7.23225 with the FLIM add-on. PMNs in TEM were identified as

those observed in a PECAM ring. An initial image was acquired (using low laser intensity to limit photobleaching) to orient the field and document the PMN position relative to the PECAM construct. A second FLIM image was acquired with only one detector set to detect TFP fluorescence at 460-500 nm (gain 190) and a zoom factor of 8.25 and speed of 100 to produce a 53.68 x 53.68 μm (105.05 nm/pixel, pixel dwell time 15.39 μs). To acquire sufficient number of photons for analysis, 60 frame repetitions were collected for each TEM event. Regions of interest corresponding to the pixels immediately surrounding the TEM event/ring were compared to the junctional regions immediately adjacent to the TEM event. Preliminary lifetime analysis for regions of interest showed that in all images, the data most closely matched a two-component exponential fit, possibly indicating the simultaneous acquisition of the emission of the two fluorophores in the FRET pair. As such, lifetimes were calculated by fitting the recorded lifetimes to a bi-exponential curve to separate the two components and their corresponding lifetimes. The component corresponding to TFP lifetime was always the major population (both in amplitude and intensity). To control for autofluorescence of the endothelial cells or spillover of fluorescence from the neutrophil cell tracker dye we collected FLIM images at the plane of the migrating neutrophils on endothelial cells that lack any PECAM construct. These images had almost no signal under the conditions used to collect the FLIM data suggesting that there was little need to correct for these other possible sources of photons.

Live cell calcium imaging—HUVEC were grown on fibronectin-coated Mattek dishes for three days with regular media and then overnight with low serum (1%) media. They were then loaded with Fluo-4 (2.5 μM , reconstituted in 20% pluronic acid in DMSO) and probenecid (2.5 mM) for 40 min at 37°C. Monolayers were then washed three times with conditioned low serum media and imaged with a 20x water immersion lens on the spinning disk microscope described above. Images of random fields were acquired briefly before the addition of histamine (10 μM final from a 10 mM stock), YODA1 (10 μM final from a 10 mM stock), or DMSO control. Monolayers were imaged continuously during the stimulation. Images shown were processed identically with minimal linear contrast adjustment and have not been corrected for photobleaching.

Orbital Shear Stress assay and orientation quantitation—HUVEC were plated on six-well glass bottom plates with #1.5 high performance cover glass (Cellvis; Sunnyvale, CA) that were pre-coated with gelatin (Cell Biologics Inc., Chicago, IL). Cultures were maintained in Gibco medium 199 supplemented with 20% heat-inactivated human serum. Once confluent, cells were incubated with growth medium containing 4% Dextran (Mr 450,000-650,000; Sigma-Aldrich; St Louis, MO) for 1 hour. Orbital shear stress was applied to confluent cultures by positioning plates on a Benchmark Orbi Shaker Jr (Benchmark Scientific Inc. Edison, NJ) for 48 hours at 37°C in a 5% CO₂ incubator, set at a rotational frequency rate of 130 RPM. At this setting, the shear stress at the periphery of the wells is approximately 11.5 dynes/cm² as previously described in ¹⁶. Cell-cell junctions were labeled live with anti-human VE-cadherin monoclonal antibody conjugated to Dylight 488 (clone hec1-488) for 15 min. Cells were rinsed with 1X Dulbecco's phosphate-buffered saline (DPBS) with calcium and magnesium and fixed with 2% paraformaldehyde for 10 min at room temperature. To visualize the actin cytoskeleton, cells were permeabilized with

0.1% Triton-X-100 for 5 min at room temperature and actin filaments were labeled with phalloidin conjugated to DyLight 550. Images were taken on a Perkin Elmer Ultraview VoX Confocal Imaging system CSU-XI, with an Olympus LUCPlanFL 20X/0.45 NA.

Transendothelial migration assays—TEM assays were performed on monolayers grown on collagen substrates as previously described⁵² with the following modifications. Where indicated, HUVEC were preincubated with SU1498 (10 μ M for 20 min), U73122 (20 μ M for 30 min), BAPTA-AM (20 μ M for 40 min), PP2 (5 μ M for 10 min), PP3 (5 μ M for 10 min), or blocking PECAM antibody hec7 (20 mg/ml for 60 min) in conditioned media, and washed briefly twice before the addition of leukocytes. For experiments blocking VEGF activity, the assay was performed with 50 ng/ml anti-VEGF antibody in the media. Assays with PBMCs were allowed 1 h to complete transmigration whereas PMNs were allowed 20 min. Monolayers were washed with PBS and 1 mM EDTA or just PBS for PBMCs and PMNs, respectively. Monolayers were then fixed, stained with modified Wright-Giemsa, and scored for leukocytes above and below as described previously⁵². In the experiments of Fig. 1, to overcome a block to PECAM cross-linking antibody (F(ab')₂ fragments of Goat anti-mouse IgG) were added for the last 20 min or 10 min for PBMCs or PMNs, respectively, of the assay as we had done previously to overcome a block of CD99⁵⁶. Hyp9 or YODA1 was added to final concentrations of 10 μ M for the last 5 min of the TEM assay. The targeted recycling assay were performed exactly as describing previously²³ on monolayers prepared with the indicated shRNA depletion and reexpression constructs described above. PMNs were allowed to migrate for 6 min for the targeted recycling assay. For treatment eluate controls, TEM was conducted as described above. At the end of the assay, the supernatant (eluate) was collected from each well, centrifuged for one minute at max speed to pellet non-adherent cells. 80 μ l of the eluate was collected and mixed with 20 μ l of fresh PMNs (or PBMCs, as indicated) and added to fresh monolayers. TEM was again allowed to proceed for 20 min or 1 h for PMNs and PBMCs, respectively, and fixed and scored as described above.

Lung Leukocyte Recruitment Assay—Inflammation of the alveolar airspace was induced with a 50 μ l instillation of 0.1 N HCl. Mice were anesthetized with 3% isoflurane mixed with room air until breathing deeply. They were intubated and instilled with two aliquots of 25 μ l 0.1 N HCl two minutes apart. Mice were placed on a heating pad to recover. 24 h after instillation, mice were sacrificed with an overdose of Avertin (Thermo Scientific Chemicals; Haverhill, MA). The lungs were immediately exposed via removal of the chest plate, and bronchoalveolar lavage (BAL) was performed with 700 μ l of sterile 0.1 M EDTA in 1x DPBS via tracheostomy. Lavage fluid was injected and removed to wash the lungs three times with a 1ml slip-tip syringe attached to a 20 G 1/2" Luer stub (Instech; Plymouth Meeting, PA). Live leukocytes in each BAL were counted with a hemacytometer and 200 μ l of each BAL was spun onto a slide at 500 rpm for 5 minutes using a Shandon Cytospin 3 (Thermo Fisher Scientific; Waltham, MA). Slides were stained with a modified Wright-Giemsa stain and mounted with Permount. Leukocyte quantification was performed on a Nikon Eclipse E800.

Intravital microscopy and croton oil dermatitis—In vivo experiments were performed as previously described³⁰. To induce Cre activity for *VEGFR2* deletion in endothelial cells, tamoxifen was administered via intraperitoneal injection (100µl per injection, 20 mg/ml tamoxifen dissolved in corn oil) once every 24 hours for five consecutive days. Mice were allowed to recover for two weeks before being used in experiments. Littermate controls (with only corn oil injection) were used where indicated.

QUANTIFICATION AND STATISTICAL ANALYSIS

Experiments with more than two conditions were first analyzed with one-way ANOVA to determine if the group contained at least one mean that was statistically different from the others. The specific condition that was statistically significant was then determined using Student's t-test pairwise for each combination. A Bonferroni correction was done to account for multiple observations. Asterisks *, **, and *** denote p-values of <0.05, <0.01, and <0.001, respectively.

Supplementary Material

Refer to Web version on PubMed Central for supplementary material.

Acknowledgements

We would like to thank Clifford D. Carpenter and Lily A. Miller for assistance with experiments and editing the manuscript. We are grateful to Martin Schwartz (Yale Medical School) for the PECAM tension sensor constructs. We thank Ralf Adams (Max Planck Institute) for the *Cdh5-CreERT2* mice and Susan Quaggin (Northwestern) the *VEGFR2^{flox/flox}* mice. Expert technical guidance for Fluorescence Lifetime Imaging Microscopy was provided by the Northwestern University Center for Advanced Microscopy; DNA sequencing was performed by the NUSeq Core Facility, both generously supported by NCI CCSG P30 CA060553 awarded to the Robert H Lurie Comprehensive Cancer Center. We would also like to thank the Sidney & Bess Eisenberg Memorial Fund for partially covering publication costs. This work was supported by NIH F31 HL131355 (to N.S.R.), Alpha Omega Alpha Carolyn L. Kuckein Student Research Fellowship, and F30 HL134202 (to P. J. D), and R01 HL064774, R01 HL046849, and R35 HL155652 (to W.A.M.)

Inclusion and Diversity

One or more of the authors of this paper self-identifies as an underrepresented ethnic minority in their field of research or within their geographical location. One or more of the authors of this paper self-identifies as a gender minority in their field of research. One or more of the authors of this paper self-identifies as living with a disability.

References

1. Huang AJ, Manning JE, Bandak TM, Rataou MC, Hanser KR, and Silverstein SC (1993). Endothelial cell cytosolic free calcium regulates neutrophil migration across monolayers of endothelial cells. *J. Cell Biol* 120, 1371–1380. [PubMed: 8449983]
2. Muller WA, Weigl SA, Deng X, and Phillips DM (1993). PECAM-1 is required for transendothelial migration of leukocytes. *J Exp Med* 178, 449–460. 10.1084/jem.178.2.449. [PubMed: 8340753]
3. Weber EW, Han F, Tauseef M, Birnbaumer L, Mehta D, and Muller WA (2015). TRPC6 is the endothelial calcium channel that regulates leukocyte transendothelial migration during the inflammatory response. *J Exp Med* 212, 1883–1899. 10.1084/jem.20150353. [PubMed: 26392222]
4. Dalal PJ, Sullivan DP, Weber EW, Sacks DB, Gunzer M, Grumbach IM, Heller Brown J, and Muller WA (2021). Spatiotemporal restriction of endothelial cell calcium signaling is required

during leukocyte transmigration. *J Exp Med* 218, e20192378. 10.1084/jem.20192378. [PubMed: 32970800]

5. Tzima E, Irani-Tehrani M, Kiosses WB, Dejana E, Schultz DA, Engelhardt B, Cao G, DeLisser H, and Schwartz MA (2005). A mechanosensory complex that mediates the endothelial cell response to fluid shear stress. *Nature* 437, 426–431. [PubMed: 16163360]
6. Grashoff C, Hoffman BD, Brenner MD, Zhou R, Parsons M, Yang MT, McLean MA, Sligar SG, Chen CS, Ha T, and Schwartz MA (2010). Measuring mechanical tension across vinculin reveals regulation of focal adhesion dynamics. *Nature* 466, 263–266. 10.1038/nature09198. [PubMed: 20613844]
7. Conway DE, Breckenridge MT, Hinde E, Gratton E, Chen CS, and Schwartz MA (2013). Fluid shear stress on endothelial cells modulates mechanical tension across VE-cadherin and PECAM-1. *Curr Biol* 23, 1024–1030. 10.1016/j.cub.2013.04.049 S0960-9822(13)00490-9 [pii]. [PubMed: 23684974]
8. Alam MS (2018). Proximity Ligation Assay (PLA). *Curr Protoc Immunol* 123, e58. 10.1002/cpim.58. [PubMed: 30238640]
9. Bhattacharya R, Kwon J, Li X, Wang E, Patra S, Bida JP, Bajzer Z, Claesson-Welsh L, and Mukhopadhyay D (2009). Distinct role of PLCbeta3 in VEGF-mediated directional migration and vascular sprouting. *J Cell Sci* 122, 1025–1034. 10.1242/jcs.041913. [PubMed: 19295129]
10. Sekiya F, Poulin B, Kim YJ, and Rhee SG (2004). Mechanism of tyrosine phosphorylation and activation of phospholipase C-gamma 1. Tyrosine 783 phosphorylation is not sufficient for lipase activation. *J Biol Chem* 279, 32181–32190. 10.1074/jbc.M405116200. [PubMed: 15161916]
11. Chen D, and Simons M (2021). Emerging roles of PLCgamma1 in endothelial biology. *Sci Signal* 14, eabc6612. 10.1126/scisignal.abc6612. [PubMed: 34344833]
12. Takahashi T, Yamaguchi S, Chida K, and Shibuya M (2001). A single autophosphorylation site on KDR/Flk-1 is essential for VEGF-A-dependent activation of PLC-gamma and DNA synthesis in vascular endothelial cells. *EMBO J* 20, 2768–2778. 10.1093/emboj/20.11.2768. [PubMed: 11387210]
13. Sase H, Watabe T, Kawasaki K, Miyazono K, and Miyazawa K (2009). VEGFR2-PLCgamma1 axis is essential for endothelial specification of VEGFR2+ vascular progenitor cells. *J Cell Sci* 122, 3303–3311. 10.1242/jcs.049908. [PubMed: 19706681]
14. Albarran-Juarez J, Iring A, Wang S, Joseph S, Grimm M, Strilic B, Wettschureck N, Althoff TF, and Offermanns S (2018). Piezo1 and Gq/G11 promote endothelial inflammation depending on flow pattern and integrin activation. *J Exp Med* 215, 2655–2672. 10.1084/jem.20180483. [PubMed: 30194266]
15. Newman PJ, and Newman DK (2003). Signal Transduction Pathways Mediated by PECAM-1: New Roles for an Old Molecule in Platelet and Vascular Cell Biology. *Arterioscler Thromb Vasc Biol* 23, 953–964. [PubMed: 12689916]
16. Dardik A, Chen L, Frattini J, Asada H, Aziz F, Kudo FA, and Sumpio BE (2005). Differential effects of orbital and laminar shear stress on endothelial cells. *J Vasc Surg* 41, 869–880. 10.1016/j.jvs.2005.01.020. [PubMed: 15886673]
17. Lou O, Alcaide P, Luscinskas FW, and Muller WA (2007). CD99 is a key mediator of the transendothelial migration of neutrophils. *J Immunol* 178, 1136–1143. 10.4049/jimmunol.178.2.1136. [PubMed: 17202377]
18. Gonzalez AM, Cyrus BF, and Muller WA (2016). Targeted Recycling of the Lateral Border Recycling Compartment Precedes Adherens Junction Dissociation during Transendothelial Migration. *Am J Pathol* 186, 1387–1402. 10.1016/j.ajpath.2016.01.010. [PubMed: 26968345]
19. Arif N, Zinnhardt M, Nyamay'Antu A, Teber D, Bruckner R, Schaefer K, Li YT, Trappmann B, Grashoff C, and Vestweber D (2021). PECAM-1 supports leukocyte diapedesis by tension-dependent dephosphorylation of VE-cadherin. *EMBO J* 40, e106113. 10.15252/embj.2020106113. [PubMed: 33604918]
20. Coon BG, Baeyens N, Han J, Budatha M, Ross TD, Fang JS, Yun S, Thomas JL, and Schwartz MA (2015). Intramembrane binding of VE-cadherin to VEGFR2 and VEGFR3 assembles the endothelial mechanosensory complex. *J Cell Biol* 208, 975–986. 10.1083/jcb.201408103. [PubMed: 25800053]

21. Warren CM, Ziyad S, Briot A, Der A, and Iruela-Arispe ML (2014). A ligand-independent VEGFR2 signaling pathway limits angiogenic responses in diabetes. *Sci Signal* 7, ra1. 10.1126/scisignal.2004235. [PubMed: 24399295]
22. Dasgupta B, and Muller WA (2008). Endothelial Src kinase regulates membrane recycling from the lateral border recycling compartment during leukocyte transendothelial migration. *Eur. J. Immunol* 38, 3499–3507. doi: 10.1002/eji.200838605. [PubMed: 18991269]
23. Mamdouh Z, Chen X, Pierini LM, Maxfield FR, and Muller WA (2003). Targeted recycling of PECAM from endothelial cell surface-connected compartments during diapedesis. *Nature* 421, 748–753. [PubMed: 12610627]
24. Muller WA (2011). Mechanisms of leukocyte transendothelial migration. *Annu. Rev. Pathol* 6, 323–344. 10.1146/annurev-pathol-011110-130224. [PubMed: 21073340]
25. Mamdouh Z, Kreitzer GE, and Muller WA (2008). Leukocyte transmigration requires kinesin-mediated microtubule-dependent membrane trafficking from the lateral border recycling compartment. *J Exp Med* 205, 951–966. 10.1084/jem.20072328. [PubMed: 18378793]
26. Cyrus BF, and Muller WA (2016). A Unique Role for Endothelial Cell Kinesin Light Chain 1, Variant 1 in Leukocyte Transendothelial Migration. *The American Journal of Pathology* 186, 1375–1386. 10.1016/j.ajpath.2016.01.011. [PubMed: 26994343]
27. Sullivan DP, Dalal PJ, Jaulin F, Sacks DB, Kreitzer G, and Muller WA (2019). Endothelial IQGAP1 regulates leukocyte transmigration by directing the LBRC to the site of diapedesis. *J Exp Med* 216, 2582–2601. 10.1084/jem.20190008. [PubMed: 31395618]
28. Wang Y, Nakayama M, Pitulescu ME, Schmidt TS, Bochenek ML, Sakakibara A, Adams S, Davy A, Deutsch U, Luthi U, et al. (2010). Ephrin-B2 controls VEGF-induced angiogenesis and lymphangiogenesis. *Nature* 465, 483–486. 10.1038/nature09002. [PubMed: 20445537]
29. Haigh JJ, Morelli PI, Gerhardt H, Haigh K, Tsien J, Damert A, Miquerol L, Muhler U, Klein R, Ferrara N, et al. (2003). Cortical and retinal defects caused by dosage-dependent reductions in VEGF-A paracrine signaling. *Dev Biol* 262, 225–241. 10.1016/s0012-1606(03)00356-7. [PubMed: 14550787]
30. Sullivan DP, Watson RL, and Muller WA (2016). 4D intravital microscopy uncovers critical strain differences for the roles of PECAM and CD99 in leukocyte diapedesis. *Am J Physiol Heart Circ Physiol* 311, H621–632. 10.1152/ajpheart.00289.2016. [PubMed: 27422987]
31. Bogen S, Pak J, Garifallou M, Deng X, and Muller WA (1994). Monoclonal antibody to murine PECAM-1 (CD31) blocks acute inflammation in vivo. *J Exp Med* 179, 1059–1064. 10.1084/jem.179.3.1059. [PubMed: 8113674]
32. Liao F, Ali J, Greene T, and Muller WA (1997). Soluble domain 1 of platelet-endothelial cell adhesion molecule (PECAM) is sufficient to block transendothelial migration in vitro and in vivo. *J Exp Med* 185, 1349–1357. [PubMed: 9104821]
33. Osawa M, Masuda M, Harada N, Lopes RB, and Fujiwara K (1997). Tyrosine phosphorylation of platelet endothelial cell adhesion molecule-1 (PECAM-1, CD31) in mechanically stimulated vascular endothelial cells. *Eur J Cell Biol* 72, 229–237. [PubMed: 9084985]
34. Osawa M, Masuda M, Kusano K.-i., and Fujiwara K (2002). Evidence for a role of platelet endothelial cell adhesion molecule-1 in endothelial cell mechanosignal transduction: is it a mechanoresponsive molecule? *J. Cell Biol* 158, 773–785. [PubMed: 12177047]
35. Otte LA, Bell KS, Loufrani L, Yeh JC, Melchior B, Dao DN, Stevens HY, White CR, and Frangos JA (2009). Rapid changes in shear stress induce dissociation of a G alpha(q/11)-platelet endothelial cell adhesion molecule-1 complex. *J Physiol* 587, 2365–2373. 10.1113/jphysiol.2009.172643. [PubMed: 19332487]
36. Wang S, Wang B, Shi Y, Möller T, Stegmeyer RI, Strilic B, Li T, Yuan Z, Wang C, Wettschureck N, et al. (2022). Mechanosensation by endothelial PIEZO1 is required for leukocyte diapedesis. *Blood* 140, 171–183. 10.1182/blood.2021014614. [PubMed: 35443048]
37. Chuntharpursat-Bon E, Povstyan OV, Ludlow MJ, Carrier DJ, Debant M, Shi J, Gaunt HJ, Bauer CC, Curd A, Simon Futers T, et al. (2023). PIEZO1 and PECAM1 interact at cell-cell junctions and partner in endothelial force sensing. *Commun Biol* 6, 358. 10.1038/s42003-023-04706-4. [PubMed: 37005489]

38. Schenkel AR, Mamdouh Z, and Muller WA (2004). Locomotion of monocytes on endothelium is a critical step during extravasation. *Nat Immunol* 5, 393–400. [PubMed: 15021878]
39. Shaw SK, Ma S, Kim MB, Rao RM, Hartman CU, Froio RM, Yang L, Jones T, Liu Y, Nusrat A, et al. (2004). Coordinated redistribution of leukocyte LFA-1 and endothelial cell ICAM-1 accompany neutrophil transmigration. *J Exp Med* 200, 1571–1580. [PubMed: 15611287]
40. Schenkel AR, Chew TW, and Muller WA (2004). Platelet endothelial cell adhesion molecule deficiency or blockade significantly reduces leukocyte emigration in a majority of mouse strains. *J Immunol* 173, 6403–6408. 10.4049/jimmunol.173.10.6403. [PubMed: 15528380]
41. Shaw SK, Bamba PS, Perkins BN, and Luscinskas FW (2001). Real-time imaging of vascular endothelial-cadherin during leukocyte transmigration across endothelium. *J Immunol* 167, 2323–2330. [PubMed: 11490021]
42. Schulte D, Kuppers V, Dartsch N, Broermann A, Li H, Zarbock A, Kamenyeva O, Kiefer F, Khandoga A, Massberg S, and Vestweber D (2011). Stabilizing the VE-cadherin-catenin complex blocks leukocyte extravasation and vascular permeability. *EMBO J* 30, 4157–4170. 10.1038/emboj.2011.304. [PubMed: 21857650]
43. Conway DE, and Schwartz MA (2015). Mechanotransduction of shear stress occurs through changes in VE-cadherin and PECAM-1 tension: Implications for cell migration. *Cell Adh Migr* 9, 335–339. 10.4161/19336918.2014.968498. [PubMed: 25482618]
44. Mamdouh Z, Mikhailov A, and Muller WA (2009). Transcellular migration of leukocytes is mediated by the endothelial lateral border recycling compartment. *J. Exp. Med* 206, 2795–2808. doi: 10.1084/jem.20082745. [PubMed: 19887395]
45. Feng G, Sullivan DP, Han F, and Muller WA (2015). Segregation of VE-cadherin from the LBRC depends on the ectodomain sequence required for homophilic adhesion. *J Cell Sci* 128, 576–588. 10.1242/jcs.159053. [PubMed: 25501813]
46. Dasgupta B, Dufour E, Mamdouh Z, and Muller W (2009). A novel and critical role for tyrosine 663 in PECAM trafficking and transendothelial migration. *J. Immunol* 182, 5041–5051. doi: 10.4049/jimmunol.0803192. [PubMed: 19342684]
47. Muller WA, Ratti CM, McDonnell SL, and Cohn ZA (1989). A human endothelial cell-restricted, externally disposed plasmalemmal protein enriched in intercellular junctions. *J Exp Med* 170, 399–414. 10.1084/jem.170.2.399. [PubMed: 2666561]
48. Muller WA, and Weigl SA (1992). Monocyte-selective transendothelial migration: dissection of the binding and transmigration phases by an in vitro assay. *J Exp Med* 176, 819–828. 10.1084/jem.176.3.819. [PubMed: 1512545]
49. Wright SD, Rao PE, Van Voorhis WC, Craigmyle LS, Lida K, Talle MA, Westberg EF, Goldstein G, and Silverstein SC (1983). Identification of the C3bi receptor of human monocytes and macrophages by using monoclonal antibodies. *Proceedings of the National Academy of Science* 80, 5699–5703.
50. Liao F, Huynh HK, Eiroa A, Greene T, Polizzi E, and Muller WA (1995). Migration of monocytes across endothelium and passage through extracellular matrix involve separate molecular domains of PECAM-1. *J Exp Med* 182, 1337–1343. [PubMed: 7595204]
51. Schlondorff J, Del Camino D, Carrasquillo R, Lacey V, and Pollak MR (2009). TRPC6 mutations associated with focal segmental glomerulosclerosis cause constitutive activation of NFAT-dependent transcription. *Am J Physiol Cell Physiol* 296, C558–569. 10.1152/ajpcell.00077.2008. [PubMed: 19129465]
52. Muller WA, and Luscinskas FW (2008). Assays of transendothelial migration in vitro. *Methods Enzymol* 443, 155–176. 10.1016/S0076-6879(08)02009-0. [PubMed: 18772016]
53. Muller WA, and Weigl S (1992). Monocyte-selective transendothelial migration: Dissection of the binding and transmigration phases by an in vitro assay. *J Exp Med* 176, 819–828. [PubMed: 1512545]
54. Kligys KR, Wu Y, Hopkinson SB, Kaur S, Platanias LC, and Jones JC (2012). $\alpha 6 \beta 4$ integrin, a master regulator of expression of integrins in human keratinocytes. *J Biol Chem* 287, 17975–17984. 10.1074/jbc.M111.310458. [PubMed: 22493440]
55. Zhang Y, Ma K, Sadana P, Chowdhury F, Gaillard S, Wang F, McDonnell DP, Unterman TG, Elam MB, and Park EA (2006). Estrogen-related receptors stimulate pyruvate dehydrogenase kinase

isoform 4 gene expression. *J Biol Chem* 281, 39897–39906. 10.1074/jbc.M608657200. [PubMed: 17079227]

56. Watson RL, Buck J, Levin LR, Winger RC, Wang J, Arase H, and Muller WA (2015). Endothelial CD99 signals through soluble adenylyl cyclase and PKA to regulate leukocyte transendothelial migration. *J. Exp. Med* 212, 1021–1041. 10.1084/jem.20150354. [PubMed: 26101266]

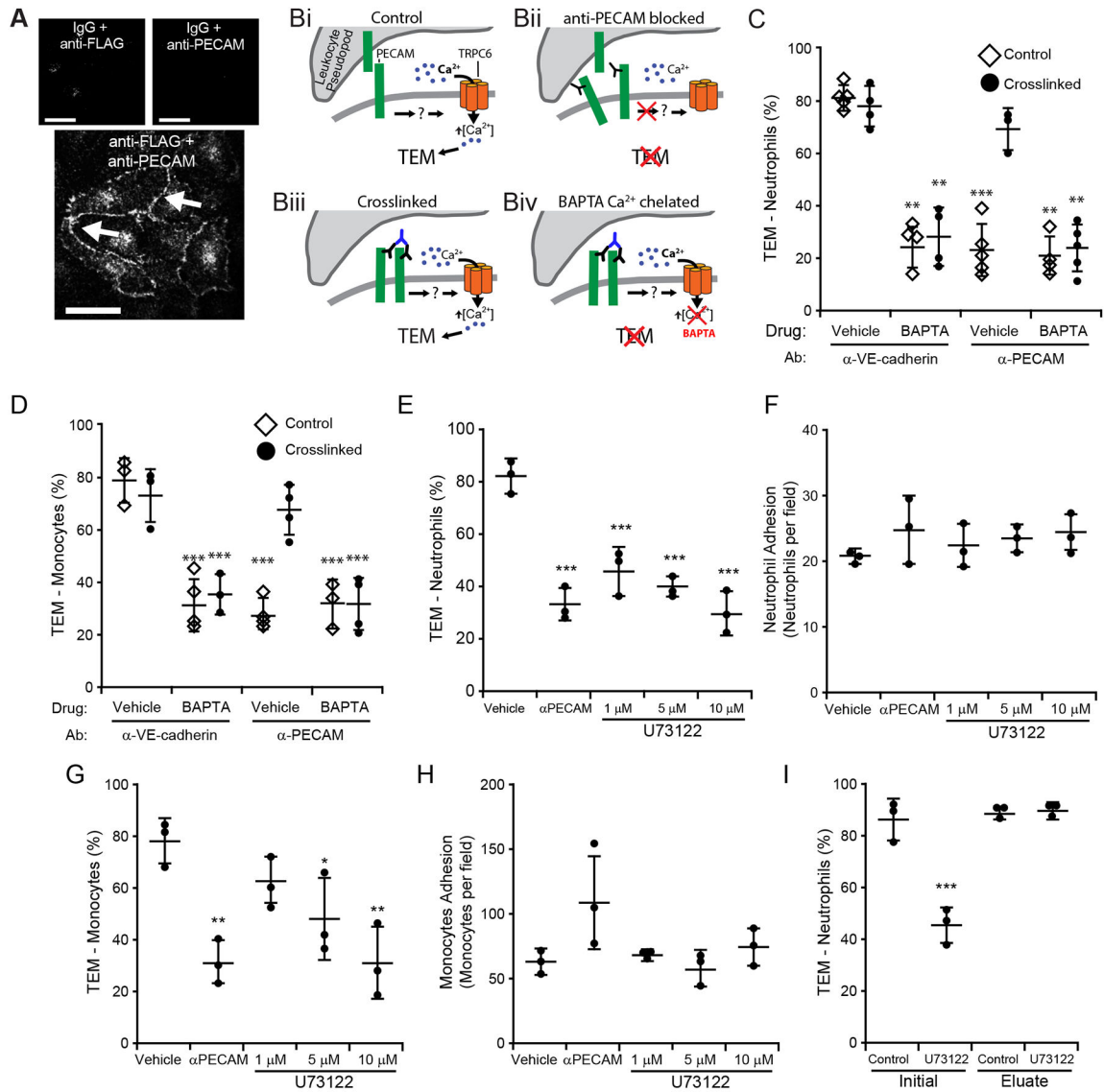


Figure 1. Cross-linking endothelial cell PECAM overcomes a PECAM antibody block in a calcium-dependent manner and leads to PLC-dependent TEM.

(A) HUVEC transfected to express FLAG-tagged TRPC6³ were incubated with anti-FLAG, anti-PECAM, or both (see Methods) then incubated with appropriate secondary antibodies and subjected to the PLA procedure. Negative controls incubated with either antibody and control IgG gave no signal (small upper panels). However, strong junctional distribution (arrows) of fluorescence was seen in the monolayers that received both antibodies, indicating that PECAM and TRPC6 closely co-localize at endothelial cell borders. Scale bar represents 50 μ m. (B) Scheme showing the methodology of the antibody blockade and crosslinking TEM assays. (Bi) Interaction of leukocyte PECAM with EC PECAM activates TRPC6 to allow $\uparrow[Ca^{2+}]_i$ and promote TEM. (Bii) Blocking anti-PECAM antibodies prevent interaction with leukocyte PECAM. No PECAM signal is generated, there is no $\uparrow[Ca^{2+}]_i$ and no TEM. (Biii) When the same PECAM antibodies are cross-linked, it mimics the engagement provided by leukocyte PECAM activating the endothelial PECAM signal,

activating TRPC6, and promoting TEM. (Biv) When the same experiment is performed in EC in which calcium concentration is buffered by BAPTA, the critical $\uparrow[\text{Ca}^{2+}]_i$ is not achieved and there is no TEM. Neutrophils (C) and monocytes (D) were added to HUVEC monolayers pretreated for 40 min with either BAPTA or vehicle and/or PECAM blocking antibodies or non-blocking anti-VE-cadherin isotype control. After 10 min (for neutrophils) or 40 min (for monocytes) goat anti-mouse F(ab')₂ was added to cross-link PECAM. Data shown represent five and four replicates for neutrophils and monocytes, respectively, with at least 300 leukocytes counted per replicate. Data are the average and standard deviation of at least three replicates per sample (typically four or five). Dose response analysis showing the effect of the broad-spectrum PLC inhibitor (U73122) on the TEM (E and G) and adhesion (F and H) of neutrophils (E and F) and monocytes (G and H). HUVEC were pretreated with either U73122 or vehicle (DMSO), or blocking anti-PECAM mAb as indicated. Quantitative data are representative of the mean and standard deviation of three experiments where at least 300 hundred leukocytes were scored per condition. Data represent the average and standard deviation of three experiments (PMN) and two experiments (monocytes). (I) Eluate control experiment (see Methods--TEM) to show that negligible U73122 elutes from the HUVEC during the experiment and does not affect the leukocytes in this TEM assay. Dots represent means of individual experiments unless otherwise indicated. Bars are the mean and standard deviation. Asterisks ** and *** denote *p*-values <0.01 and <0.001 respectively.

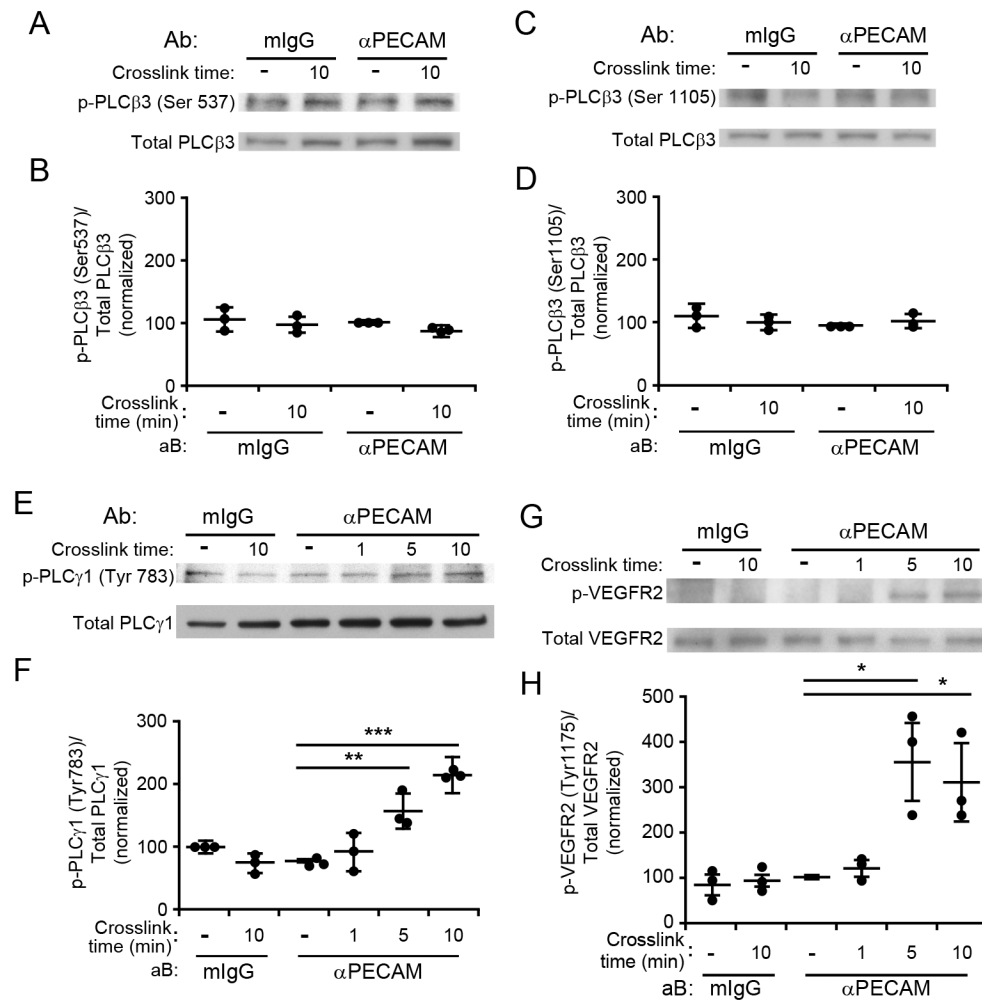


Figure 2. PECAM cross-linking induces phosphorylation of PLCγ and VEGFR2.

HUVEC monolayers were incubated with either anti-PECAM antibodies or control non-specific mouse IgG (mIgG) for 1 h and then washed and treated with secondary cross-linking antibody for the indicated time to stimulate PECAM signaling. Monolayers were then lysed and their proteins resolved using SDS-PAGE and western blotting. The phosphorylation of PLCβ3 at serines 537 (A) and 1105 (C) PLCγ1 tyrosine 783 (E), and VEGFR2 tyrosine 1175 (G) were probed using specific antibodies. Blots were then stripped and reprobed to determine total protein expression. Band intensities were quantified using densitometry and normalized to the total amount of the indicated protein (B, D, F, H). Data shown were normalized to the control (mIgG, no cross-linking) samples. Dots represent means of individual experiments unless otherwise indicated. Bars are the mean and standard deviation. Asterisks *, **, and *** denote *p*-values < 0.05, < 0.01 and < 0.001 respectively.

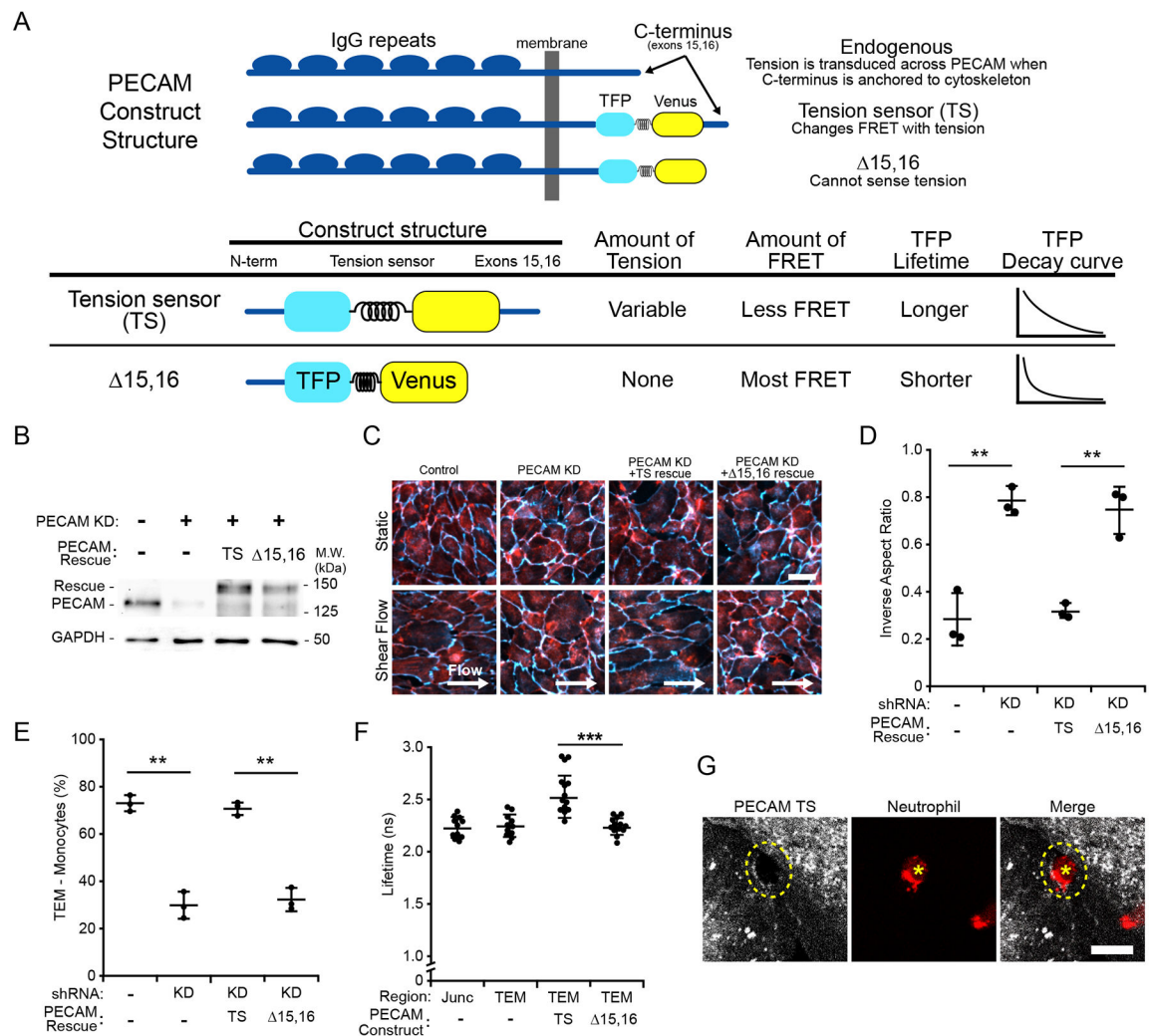


Figure 3. PECAM tension sensing is required for TEM.

(A) Schematic of PECAM tension sensing and control constructs used in this project. (B) HUVEC monolayers were transfected with PECAM shRNA followed by PECAM tension sensor (TS) and non-sensing ($\Delta 15,16$) rescue constructs as indicated. (B) Western blot analysis of transfected constructs confirms efficient protein depletion and reexpression. Samples were probed with GAPDH as a loading control. (C) Monolayers prepared as described in (B) were subjected to shear flow at 11.5 dynes/cm² for 48 h as described in the Materials and Methods. They were then fixed, stained for VE-cadherin (blue) and actin (red), and visualized using confocal microscopy. Arrow indicates direction of flow; scale bar is 100 μ m. (D) Quantitation of the inverse aspect ratio in C, where 1.0 would be a cell with equal length and width. Data are the mean and standard deviation of at least 50 cells from three separate experiments. (E) HUVEC monolayers prepared as described in B were incubated with monocytes for one hour to examine their ability to support TEM. Data shown represent the mean and standard deviation of three separate experiments with at least 300 monocytes scored per experiment. (F,G) HUVEC monolayers prepared as described above were visualized by fluorescence lifetime imaging microscopy (FLIM) measurements

during neutrophil TEM. Only monolayers expressing the tension-sensing PECAM construct showed an increase in fluorescence lifetime of TFP, indicating stretching of the PECAM molecule that corresponded to the act of TEM (F) Dots represent individual PMN/EC interactions. At least 11 were observed for each condition. (G) Image of PECAM tension sensor around a neutrophil (red; yellow asterisk) engaged in TEM. The dashed yellow circle denotes the corresponding region of interest that was measured for FLIM. Scale bar = 10 μm . Dots represent means of individual experiments unless otherwise indicated. Bars are mean \pm standard deviation. Asterisks ** and *** denote p -values <0.01 and <0.001 respectively.

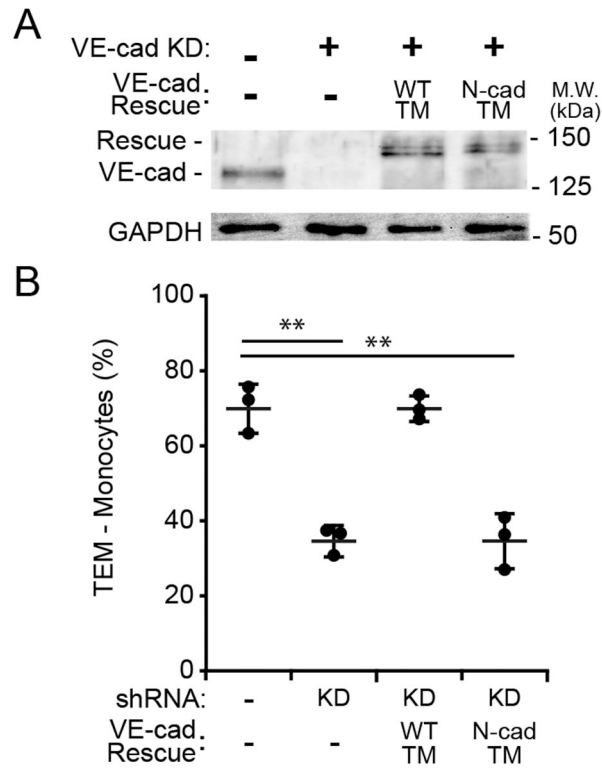


Figure 4. Efficient TEM requires the endogenous transmembrane domain of VE-cadherin. HUVEC were incubated with adenovirus expressing shRNA against VE-cadherin and then rescue constructs that expressed either wild-type VE-cadherin (WT-TM) or VE-cadherin with its transmembrane domain replaced with that of N-cadherin (N-cad-TM). (A) Representative (of 3 independent experiments) Western blot showing efficient depletion of endogenous VE-cadherin and appropriate re-expression of TM-domain constructs. (B) Quantification of TEM assays using endothelial monolayers prepared as in (A). shRNA depletion of endogenous VE-cadherin significantly impairs TEM. Re-expression of wild-type VE-cadherin restored TEM to baseline, whereas re-expression of VE-cadherin whose transmembrane domain was replaced with that of N-cadherin did not. Dots represent means of individual experiments unless otherwise indicated. Bars are mean and standard deviation from three independent experiments. Asterisks ** denote p -value <0.01 .

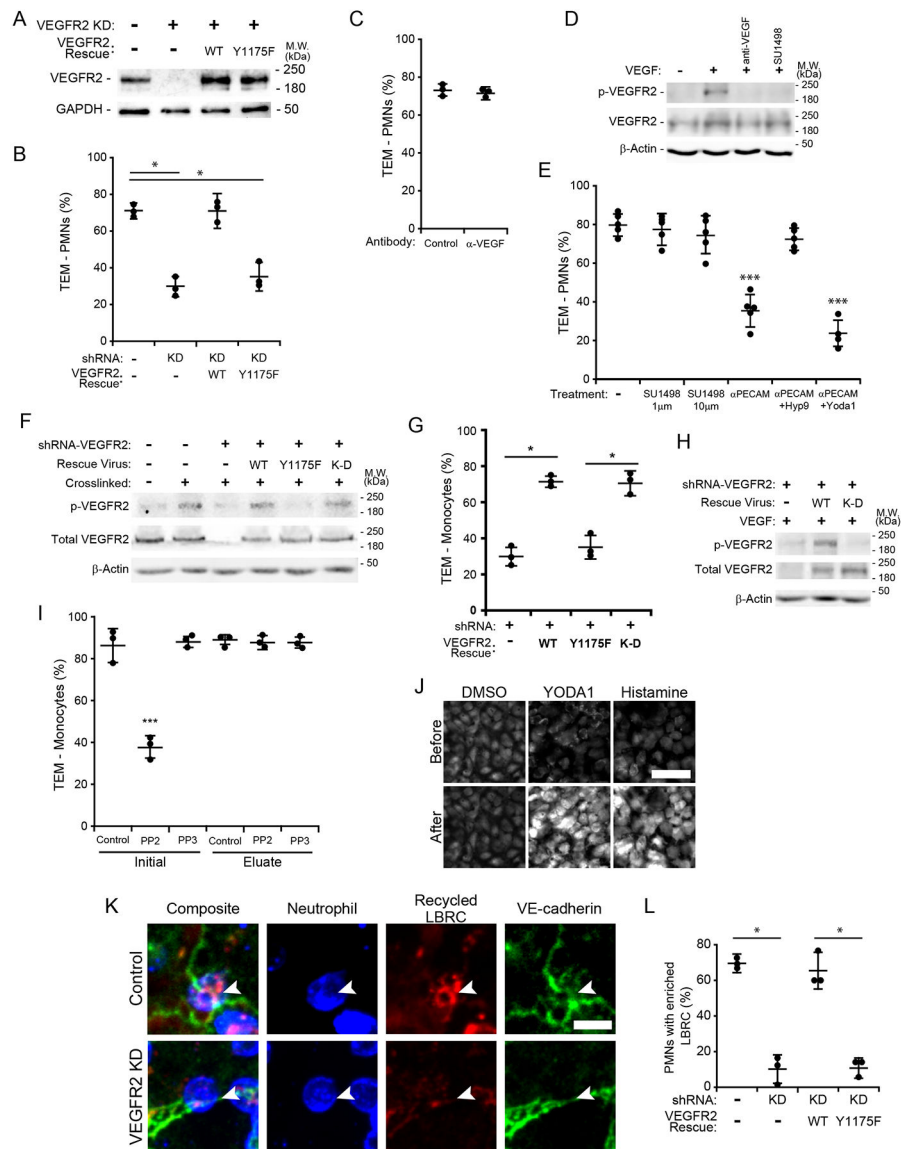


Figure 5. VEGFR2 is required for targeted recycling and TEM in a ligand-independent manner.

(A) Depletion of VEGFR2 in HUVEC using shRNA delivered by adenovirus and reconstitution of those HUVEC with wild-type VEGFR2 (WT) or VEGFR2 with tyrosine 1175 mutated to phenylalanine (Y1175F). (B) Neutrophils (PMN) subjected to transmigration assay across HUVEC monolayers expressing VEGFR2 as in panel (A). TEM is significantly diminished in the VEGFR2 depleted cells, but rescued completely when WT VEGFR2 is restored. Re-expressing VEGFR2 with the Y1175F mutation does not rescue TEM. (C) Running the TEM assay in the presence or absence of anti-VEGF antibody did not affect transmigration of PMN. (D) HUVEC serum-starved overnight then pre-incubated with 10 μ g/ml of bevacizumab, a blocking anti-VEGF antibody or 10 μ M SU1498 for 20 minutes prior to addition of VEGF (20 ng/ml). Incubation of HUVEC for 5 min. Monolayers were lysed and subjected to Western Blot for p-1175 VEGFR2, then stripped and probed for total VEGFR2. (E) TEM assays of monocytes were carried out

in the presence of SU1498 at the concentrations indicated, or hec7 (blocking anti-PECAM mAb) at 20 $\mu\text{g/ml}$ for 55 minutes. After 55 minutes, Hyp9 or YODA1 were added to the corresponding wells to a final concentration of 10 μM in the continued presence of hec7. The TEM assay was stopped at 60 min. (F) Control HUVEC monolayers or those with VEGFR2 depleted and replaced with the indicated rescue constructs (K-D = kinase dead) underwent PECAM cross-linking and blotting for phosphorylation of Y1175. Results are representative of 3 independent experiments. (G) HUVEC monolayers with VEGFR2 depleted and rescued with control virus, wild-type VEGFR2, or the indicated mutant VEGFR2 constructs were used in the TEM assay. (H) Control experiment to show that kinase dead (K-D) VEGFR2 mutant is not phosphorylated when exposed to VEGF. (I) TEM of neutrophils across HUVEC pretreated with DMSO (Control), or 5 μM PP2 or PP3 for 10 min. Eluate controls were performed as in Fig. 1I, showing that no detectable reagent eluted from the monolayers to directly affect the leukocytes. (J) HUVEC were loaded with Fluo4 and imaged live using a water-immersion lens for several minutes before and after addition of DMSO (carrier), YODA1 (10 μM), and histamine (10 μM) Still images from the live recording (Please see Supplemental Videos 1-3) are shown. Scale bar is 100 μm . (K, L) Targeted recycling assay during transmigration of PMN across control, VEGFR2 depleted and depleted→reconstituted endothelial monolayers. (K) During normal TEM (Control), the LBRC moves to surround the PMN as it transmigrates, while VE-cadherin forms a gap (arrowhead). When VEGFR2 is depleted (VEGFR2 KD), the LBRC does not move to the surface to surround the PMN and VE-cadherin remains visible under the neutrophil (arrowhead). The result is no TEM. Scale bar is 20 μm . (L) Quantification of the percent of PMN with enriched LBRC on the corresponding monolayers. Because this assay captures a snapshot in time early in the transmigration of the PMN population, most PMN have not transmigrated yet. However, the ratios of LBRC enrichment are proportional to the final TEM in this assay (panel B). Asterisks * and *** denote *p*-values of <0.05 and <0.001 respectively.

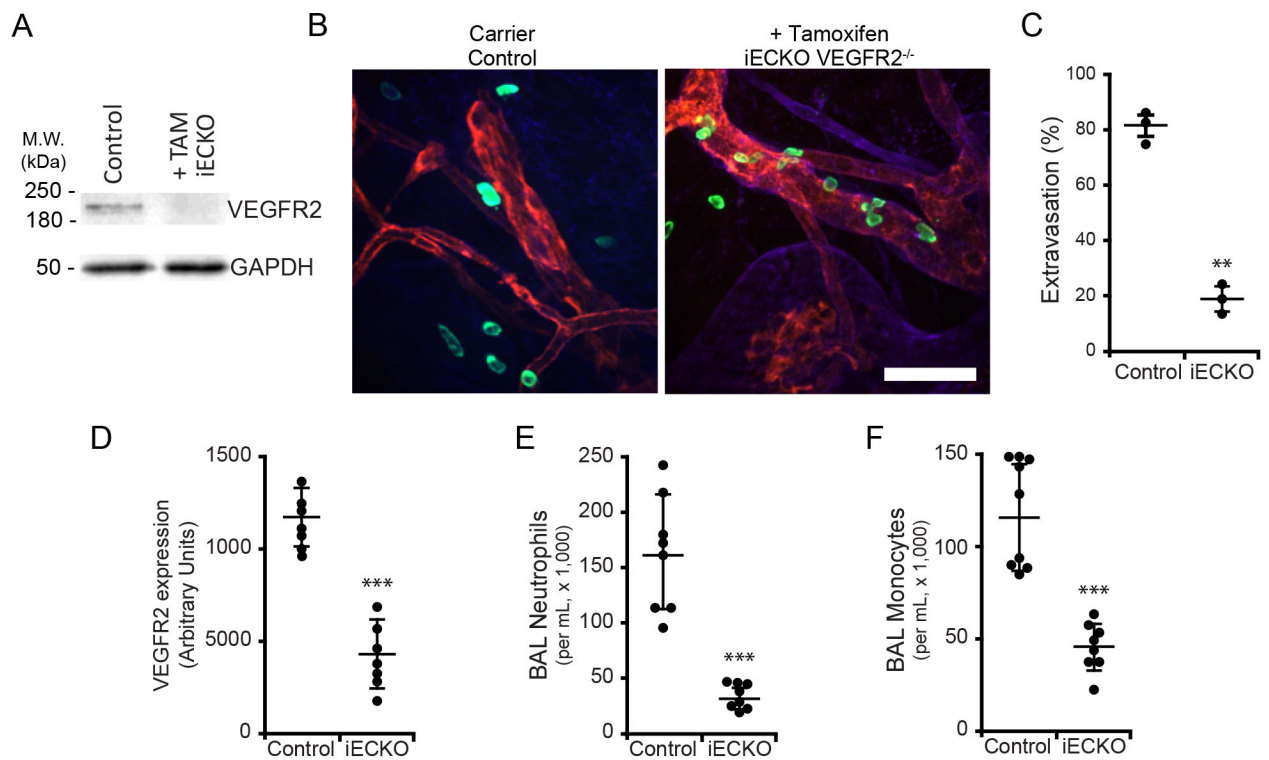


Figure 6. Endothelial-specific inducible VEGFR2 deficient mice have defective neutrophil extravasation.

(A) Inducible endothelial-specific Cre mice (*Cdh5*(PAC)-CreERT2²⁸) were mated with *Flk-1*^{fl/fl} mice²⁹ and backcrossed until homozygous for *Flk-1*^{fl/fl}. Mice were treated with tamoxifen (+TAM) in corn oil to induce deficiency of VEGFR2 selectively in endothelial cells (iECKO) or corn oil alone for 5 days, rested for at least two weeks, and then endothelial cells isolated from lungs. Lysates were probed by Western Blot for VEGFR2. (B) Mice with inducible endothelial-specific deficiency of VEGFR2 (iECKO) or littermates that received corn oil only were studied in the croton oil dermatitis model. Five hours after application of croton oil to the mouse ear skin many PMN (S100A9, green) were seen in the interstitial tissue outside of vessels (PECAM, red) and their associated basement membrane (collagen IV, blue). An equal number of PMN are recruited to the ears of inducible endothelial-specific VEGFR2 deficient mouse, but the vast majority remain within the postcapillary venules, apparently attached to the endothelium. Scale bar is 100 μ m. (C) Quantification of three independent experiments. PMN extravasation is reduced from 80% to 20%. Asterisk denotes p -value <0.01 . (D) Inducible endothelial-specific VEGFR2 deficient mice bred as in (A) were fed Tamoxifen Chow or normal chow for at least 20 days, then PBS (Control) or 0.1N HCl was instilled into their lungs via the trachea. (See Methods.) Twenty four hours later, mice were euthanized and bronchoalveolar lavage (BAL) fluid collected from each mouse. The lungs were then harvested, extracted, and probed for VEGFR2 by Western blot. Graph (D) shows quantification of blots for 8 mice per condition. The number of neutrophils (E) and monocytes (F) was quantified from the BAL fluid. The dots represent data from individual mice in an experiment representative of three

independent experiments. Bars represent mean \pm standard deviation. Asterisks ** and *** denote p -values of <0.01 and <0.001 respectively.

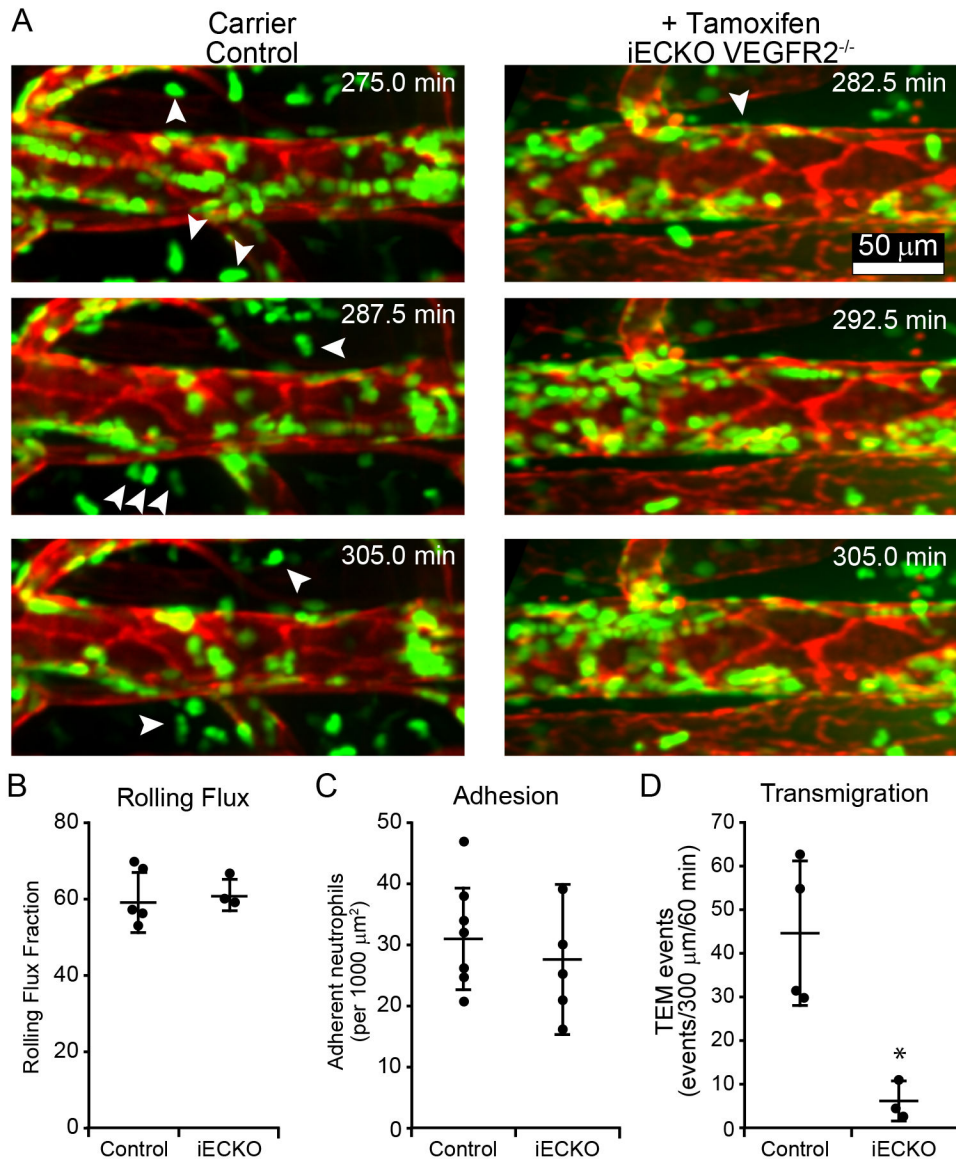


Figure 7. Endothelial-specific inducible VEGFR2 deficient mice have defective transendothelial migration.

(A) EC-specific VEGFR2-deficient mice (iECKO) were produced as for the experiments in Fig. 6. Male mice were studied by intravital microscopy of the cremaster muscle circulation following intrascrotal injection of murine IL-1 β . Video recordings were made using a spinning disc confocal microscope as described³⁰. Shown are representative frames from Supplemental Videos 4 and 5. Circulating PMN express LysM-eGFP (green); endothelial cell borders are stained by a non-blocking mAb against mouse PECAM (red). White arrowheads point to extravasating PMN. (B – D) Quantification of rolling (B), adhesion (C), and TEM (D) from at least three independent experiments. Dots represent means of individual experiments unless otherwise indicated. Bars are the mean \pm standard deviation is shown. Only the TEM step was significantly decreased in the endothelial specific inducible VEGFR2-deficient mice. Asterisk * denotes p -value < 0.05 , scale bar = 50 μ m.

KEY RESOURCES TABLE

Reagent	Manufacturer	Catalogue Number
Mouse line LysM-GFP VEGFR2 ^{fllox/flox} Cad5-CreERT2	This study	
Antibody mouse anti-human PECAM IgG2a (clone hec7)	47	
Antibody mouse anti-human VE-cadherin (clone hec1)	48	
Antibody armenian hamster anti-mouse PECAM (clone 2H8)	40	
Antibody mouse anti-human CD18 (clone IB4)	49	
Antibody mouse anti-human PECAM antibody (clone P1.1)	50	
Antibody mouse anti-human β -actin (clone AC-74)	Millipore Sigma	A2228
Antibody rat anti-mouse PECAM (clone 390)	Millipore Sigma	CBL1337
Antibody Rabbit anti-mouse collagen IV (clone 2B10)	Abcam	ab19808
Antibody rat anti-mouse myeloid-related protein 14 (MRP14) (clone 2B10)	Abcam	ab105472
Antibody anti-FLAG	Sigma-Aldrich	A9594
Goat Anti-Rabbit IgG*488	Jackson ImmunoResearch Laboratories	111-545-144
Goat Anti-Mouse IgG*RRX	Jackson ImmunoResearch Laboratories	115-295-003
Goat Anti-Mouse IgG*488	Jackson ImmunoResearch Laboratories	115-545-003
Goat Anti-Mouse IgG*RRX	Jackson ImmunoResearch Laboratories	115-295-003
Alexa Fluor [®] 647 AffiniPure Goat Anti-Rabbit IgG	Jackson ImmunoResearch Laboratories	111-605-144
Antibody rabbit anti human PLC γ 1	Cell Signaling	D9H10
Antibody rabbit anti-human phospho-PLC γ 1-Tyr783	Cell Signaling	2821S
PLCbeta3 (D9D6S) Rabbit mAb	Cell Signaling	14247
PLCbeta3 (D9D6S) Rabbit mAb	Cell Signaling	2481s
Phospho-PLCbeta3 (Ser1105) Antibody	Cell Signaling	2484s
Antibody rabbit anti-human VEGFR2	Cell Signaling	2479S
Antibody rabbit anti-human phospho-VEGFR2-Tyr1175	Cell Signaling	2478L
Normal Mouse Serum	Jackson ImmunoResearch Laboratories	015-000-120
Normal Goat serum	Jackson ImmunoResearch Laboratories	005-000-121
Peroxidase AffiniPure Goat Anti-Mouse IgG (H+L)	Jackson ImmunoResearch Laboratories	115-035-003
Goat anti-Rabbit IgG (H+L) Poly-HRP	Thermo Fisher Scientific	32260
DyLight [™] 550 Antibody Labeling Kit	Thermo Fisher Scientific	PI84530
Recombinant Human TNF-alpha Protein	R & D Systems	210-TA-020
Human VEGF-165	Shenandoah Biotechnology, Inc.	100-44-10ug
YODA1	Bio-Techne	5586
SU1498	Cayman Chemicals	SU1498
VEGFR2-mCherry plasmid	Addgene	plasmid#108854
VE-cadherin-GFP pENTR4 plasmid	18	
PECAM tension sensor plasmid	7	
PECAM tension sensor-tailless plasmid	7	
pAd-DEST-PL plasmid	Thermo Fisher Scientific	V49420

Reagent	Manufacturer	Catalogue Number
pAD-DEST-CMV-V5 plasmid	Thermo Fisher Scientific	V49320
pENTR4 entry vector	Invitrogen Corp.	11818-010
pENTR/U6 BlockiT plasmid	Invitrogen Corp.	K494500
TRPC6-wildtype-Nterm-FLAG-tagged plasmid	51	
TRPC6-Dominant negative-Nterm-FLAG-tagged plasmid	51	
Duolink Proximity Ligation Assay kit	Millipore Sigma	DUO92101-1KT
Protease inhibitor cocktail	Sigma-Aldrich	P8340
Bovine Serum Albumin, Fraction V	Thermo Fisher Scientific	BP1600-100
Mattek coverslip dishes	MATTEK CORP.	P35GC-1.5-10-C
Velocity software	Perkin Elmer	version #####
FIJI imageJ	NIH	version 1.53q
Fluo-4 calcium indicator	Life Technologies	F-14201
Histamine dihydrochloride	Millipore Sigma	H7250-10MG
Hyp9	Millipore Sigma	H9791-25MG
BAPTA-AM	Abcam, Inc.	ab120503
U-73122 hydrate	Millipore Sigma	U6756-5MG
Corn oil	Millipore Sigma	C8267-500ml
Tamoxifen	Millipore Sigma	Envigo Intl.
Tamoxifen chow	Millipore Sigma	TD.130855
Six-well glass bottom plates	Cellvis	P06-1.5H-N
GELATIN-BASED COATING	Cell Biologics	6950
Gibco Medium 199, Hank's	Thermo Fisher Scientific	12350-039
Orbi Shaker Jr	Benchmark Scientific Inc.	BT302
PP2, Src and RIP2 kinase inhibitor	Abcam, Inc.	ab120308
PP3, Negative control for PP2	Abcam, Inc.	ab120617
Lipofectamine 2000	Thermo Fisher Scientific	11668-027
AffiniPure Goat Anti-Armenian Hamster IgG	Jackson ImmunoResearch Lab Inc	127-005-160